

REVIEW

Purely organic room temperature phosphorescent materials toward organic light-emitting diodes

Hui Li  | Cheng Chen | Zongji Ye | Kai Feng | Jiani Huang | Gaozhan Xie | Ye Tao

State Key Laboratory of Organic Electronics and Information Displays & Institute of Advanced Materials (IAM), Nanjing University of Posts & Telecommunications, Nanjing, China

Correspondence

Ye Tao and Gaozhan Xie.
Email: iamytao@njupt.edu.cn and iangzxie@njupt.edu.cn

Funding information

the Open Research Fund of Songshan Lake Materials Laboratory, Grant/Award Number: 2022SLABFN16; National Natural Science Foundation of China, Grant/Award Number: 22075149, 22322106, 62075102, 22105104 and 6228810; Project of State Key Laboratory of Organic Electronics and Information Displays, Grant/Award Number: GDX2024010002

Abstract

Purely organic room temperature phosphorescence (RTP) materials have shown broad application prospects in organic light-emitting diodes (OLEDs) due to their theoretical 100% exciton utilization, cost-effectiveness, and flexibility. In recent years, with the deepening of research, various luminescent mechanisms have been proposed, and RTP materials have made significant progress, which have been effectively applied to OLEDs. This article comprehensively reviews the research progress of RTP materials in OLEDs and introduces the development of a series of high-efficiency RTP materials from the perspective of molecular design strategies and photophysical properties. These conclusions draw a roadmap to address the inherent challenges in utilizing organic RTP materials to specifically advance the investigation of OLEDs.

KEYWORDS

organic light-emitting diodes, room temperature phosphorescence, triplet excitons

1 | INTRODUCTION

Purely organic room temperature phosphorescence (RTP) materials have garnered considerable attention, owing to their facilitated luminescence through the utilization of triplet exciton radiation and rich excited state properties. These attributes have rendered RTP materials highly versatile, enabling applications across diverse domains such as bio-imaging, information encryption, fingerprint identification and organic light-emitting diodes (OLEDs). In the realm of biological imaging, the incorporation of RTP materials presents a promising avenue to enhance the sensitivity and precision of imaging techniques.^{1–5} For information encryption, the

distinctive fluorescence and RTP properties introduce novel possibilities for anti-counterfeiting and identification purposes.^{6–10} For fingerprint identification, RTP materials can effectively eliminate the disturbing background fluorescence.^{11–13} Particularly, the integration of RTP materials into the OLED sector opens up new vistas for the development of more efficient and sustainable organic light sources.^{14,15} The ongoing research advancements in the domain of RTP-based OLEDs have generated substantial interest. Therefore, the demand for the development of high-performance RTP OLEDs has dramatically aroused researchers' interest in exploring the excellent RTP materials with relatively strong inter-system crossing (ISC) effects and reduced triplet exciton

This is an open access article under the terms of the [Creative Commons Attribution](https://creativecommons.org/licenses/by/4.0/) License, which permits use, distribution and reproduction in any medium, provided the original work is properly cited.

© 2024 The Author(s). FlexMat published by John Wiley & Sons Australia, Ltd on behalf of Nanjing University of Posts & Telecommunications.

deactivation, which are the two critical prerequisites for RTP materials.^{16–18}

Efficient organic RTP materials can be obtained through reasonable molecular design strategies. To promote the ISC process, various strategies, including the introduction of heavy atoms,^{19–22} narrowing the energy gap,^{23,24} hyperfine coupling,^{25,26} heteroatom engineering,^{27–31} etc., have been proposed. To suppress the non-radiative deactivation of triplet excitons, rigid environments are usually constructed to protect the chromophore from oxygen quenching and to suppress molecular vibrations through H-aggregation engineering,^{32,33} crystallization,^{34–36} host-guest systems,^{37–41} and polymerization.^{29,42,43} As the field advances, significant breakthroughs in the development of RTP materials could be anticipated, heralding a new era of organic optoelectronic materials with substantial effects on the evolution of organic electronics.

Figure 1 showcases the key milestones in the development of organic RTP OLEDs. In 2013, Bergamini et al. employed RTP materials for the fabrication of OLEDs.⁴⁴ In 2016, Anzenbacher and colleagues developed materials with both fluorescence and RTP emissions in solution and solid states.⁴⁵ In the same year, Adachi et al. utilized a host-guest strategy to construct an afterglow OLED, observing blue fluorescence and green long-persistent luminescence during and after the removal of the applied voltage.⁴⁶ In 2018, He et al. synthesized RTP polymers containing bromine (Br) atoms and fabricated the OLEDs, which showed a maximum brightness of 194 cd/m².⁴⁷ In 2019, Wang and coworkers developed an organic RTP material, achieving highly efficient OLEDs with a maximum external quantum efficiency (EQE) of 11.5%.⁴⁸ In 2019, Zhang et al. designed a series of molecules with aggregation-induced phosphorescence (AIP) properties, endowing the OLEDs with a maximum EQE of

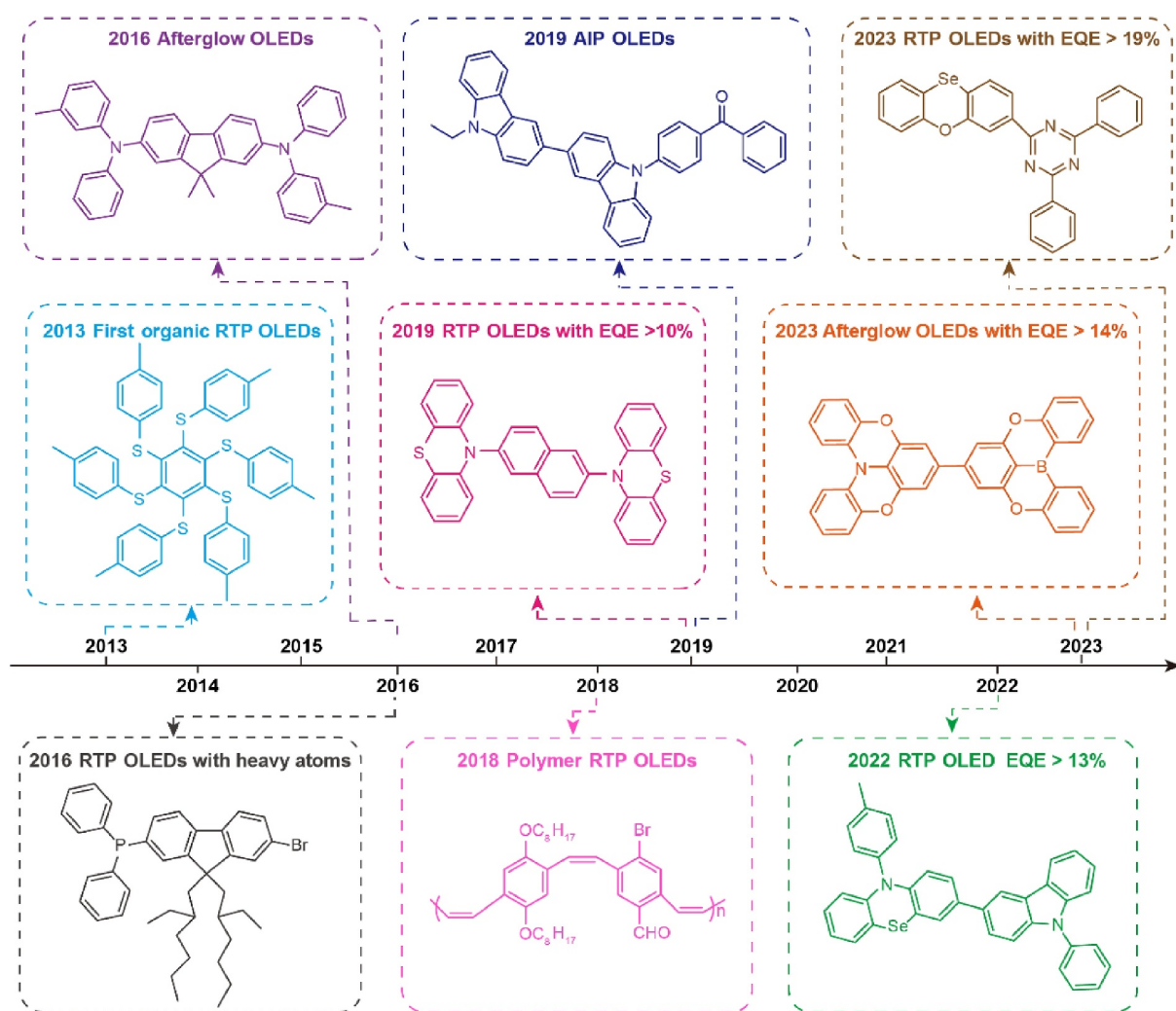


FIGURE 1 Development of organic RTP materials for OLED applications. OLED, organic light-emitting diodes; RTP, room temperature phosphorescence.

5.8% and relatively low efficiency roll-off.⁴⁹ In 2022, Lee and colleagues achieved an impressive OLED showing a maximum EQE of 13.2% using emissive RTP materials.⁵⁰ In 2023, Su's group reported RTP materials with enhanced spin-orbit coupling (SOC) by utilizing selenium (Se) atoms, conferring a record-breaking EQE of 19.5% for RTP OLEDs.⁵¹ In the same year, the same team also succeeded in designing and fabricating the afterglow OLED device based on polycyclic aromatic hydrocarbons, achieving an impressively high EQE of 14.7%.⁵²

In short, the development of RTP OLEDs has just begun, and further research is urgently needed. Considering the swift progress in this domain, it is crucial to methodically explore and summarize the RTP mechanism, design principles, and OLED applications, as well as shed light on the future directions of RTP materials. In this review, the basic concept and main process of RTP are introduced, with a focus on ISC enhancement and the suppression of non-radiative transitions. Subsequently, the application of RTP materials in OLEDs is discussed. Moreover, the conclusion and perspective for RTP materials in OLED are given. This review would provide researchers with a holistic view and enable newcomers to rapidly grasp the significance of this dynamic area.

2 | MAIN PROCESS OF PHOSPHORESCENCE

As shown in Figure 2, the radiative transitions of the exciton from the lowest singlet state (S_1) to the ground state (S_0) produce fluorescence, and the radiative transitions of the exciton from the lowest triplet state (T_1) to S_0 generate phosphorescence. The T_1 excitons can be formed by the ISC from S_1 to highly excited triplet exciton (T_n), followed by the fast internal conversion (IC) from T_n to T_1 according

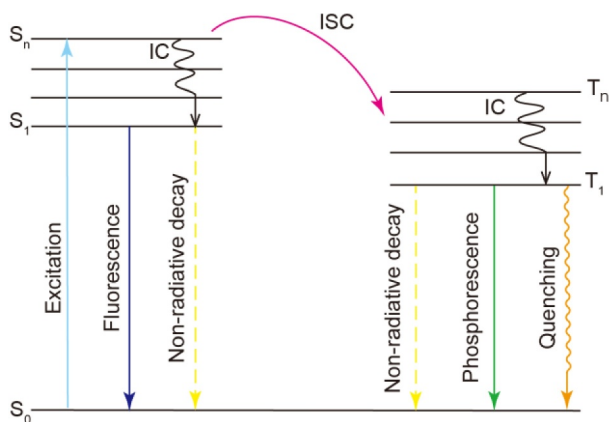


FIGURE 2 Jablonski diagrams of key photophysical processes in organic molecules.

to Kasha's rule. The phosphorescence process is much slower compared to fluorescence due to the transition from T_1 to S_0 is inherent in spin-forbidden purely organic materials, which makes the lifetime of phosphorescence much longer than that of fluorescence. The lifetime (τ_p) and the quantum yield (Φ_p) of the phosphorescence can be defined by the following equations:

$$\tau_p = \frac{1}{k_p + k_{nr} + k_q} \quad (1)$$

$$\Phi_{ISC} = \frac{k_{ISC}}{k_f + k_{nr}^f + k_{ISC}} \quad (2)$$

$$\Phi_p = \frac{\Phi_{ISC} k_p}{k_p + k_{nr}^p + k_q} \quad (3)$$

where k_f and k_{nr}^f represent the radiation and non-radiative decay rates from S_1 to S_0 , k_p , and k_{nr}^p that are the radiative and non-radiation decay rates from T_1 to S_0 , respectively. k_{ISC} is the ISC rate from S_1 to T_1 , and k_q is the quenching rate of the triplet exciton. Therefore, high k_{ISC} and $k_p > k_{nr} + k_q$ are essential for achieving efficient RTP molecules. However, the triplet excitons are easily wasted by oxygen quenching and molecular motion, which results in large $k_{nr} + k_q$, thus RTP can only be observed in inert atmospheres and/or at low temperatures. Generally, the phosphorescent quantum yield (PhQY) is low at room temperature due to the intense molecular motion. The method of obtaining efficient phosphorescence emission can be summarized as follows: (1) promoting the ISC process from S_1 to T_1 . (2) suppressing the non-radiative decay of triplet exciton.⁵³

The rate of ISC (k_{ISC}) can be expressed as:

$$k_{ISC} = \frac{2\pi}{\hbar} |\langle S | \hat{H}_{SOC} | T \rangle|^2 \sqrt{\frac{\pi}{\lambda k_B T}} \exp \left[-\frac{(\Delta E_{ST} - \lambda)^2}{4\lambda k_B T} \right] \quad (4)$$

where $\langle S | \hat{H}_{SOC} | T \rangle$ is the SOC matrix element between singlet and triplet states; k_B and T represent the Boltzmann constant and temperature, respectively; \hbar is the reduced Planck's constant; λ is the total reorganization energy; ΔE_{ST} is the energy gap between the two involved electronic states at their equilibrium geometries. Based on the equation, SOC plays a primary role in promoting the ISC process. According to the El-Sayed rule, the SOC process between the two electronic transition states is more readily available when the molecular orbital types are changed. For example, the excitons transition from $^1(\pi, \pi^*) \rightarrow ^3(n, \pi^*)$ and $^1(n, \pi^*) \rightarrow ^3(\pi, \pi^*)$ are allowed, while $^1(n, \pi^*) \rightarrow ^3(n, \pi^*)$ and $^1(\pi, \pi^*) \rightarrow ^3(\pi, \pi^*)$ are forbidden. Moreover, according to Equation (5),⁵⁴ the

main part of the spin-orbit Hamiltonian (\hat{H}_{SOC}), expressed for a single atom with a Coulombic field, is:

$$\hat{H}_{\text{SOC}} = \xi \left(\frac{Z^4}{n^3} \right) LS \propto Z^4 \quad (5)$$

where ξ is the spin-orbit coupling factor, Z is the atomic number, n is the principal quantum number, L and S are orbital angular momentum and spin angular momentum, respectively. Therefore, the SOC constant is proportional to the fourth power of the atomic number (Z^4); the introduction of heavy atoms such as Br, iodine (I), sulfur (S), and Se becomes a common strategy in the design of efficient RTP molecules.⁵⁵ Besides the heavy atom effect, a small energy gap ΔE_{ST} is also a common strategy to obtain efficient RTP molecules. Moreover, to inhibit the oxygen- and molecular motion-induced non-radiative of triplet excitons through rigidification effect, various strategies have been developed, such as crystallization,^{56–58} polymerization,^{59,60} matrix rigidification,⁶¹ host-guest doping,⁶² and metal-organic frameworks (MOFs).^{63,64} Because the rigidification effect can greatly suppress the non-radiative rate and quenching rate, the RTP lifetime and efficiency can be simultaneously enhanced. Therefore, the following parts will introduce the development of RTP molecules in OLEDs from two aspects: facilitated ISC and reduced triplet exciton deactivation.

3 | ORGANIC RTP MATERIALS FOR OLEDs

3.1 | Facilitated ISC

The facilitation of ISC, the process by which an excited electron transitions from a singlet state to a triplet state with a different spin multiplicity, is a critical factor in designing RTP materials. The promotion of ISC is challenging due to the inherently weak SOC in organic molecules. To counteract the low ISC rate, a set of methods to amplify the SOC and minimize the ΔE_{ST} have been proposed for the preparation of pure organic RTP emitters.

3.1.1 | Heavy-atom effect

The heavy-atom effect is a classic photophysical phenomenon wherein the introduction of heavy atoms into organic fluorophores would promote their SOC. At present, most conventional phosphorescent materials are metal complexes, which usually use noble heavy metals such as iridium (Ir) and platinum (Pt) to enhance SOC to produce phosphorescence. Whereas, the high costs and limited resources of the noble heavy metals prevent their further

development and practical applications. Therefore, the design and development of pure organic RTP materials are extremely attractive. In recent years, numerous organic RTP materials have been explored through the heavy-atom strategy by introducing halogen atoms, sulfur (S) and/or Se atoms into organic molecules, and then successfully used in OLEDs.

In 2016, Anzenbacher and co-workers successfully developed two RTP materials **1–2** (Figure 3) via heavy-atom strategy.⁴⁵ Due to the presence of bromine and phosphorus atoms, the RTP is remarkably enhanced, displaying both RTP emission in solid states with emission peaks at 509 and 516 nm for molecules **1** and **2** (Table 1). The RTP OLED with the structure of ITO/PEDOT:PSS/TCTA:1/TPBi/CsF/Al was prepared. In this device, poly(3,4-ethylenedioxythiophene):polystyrene sulfonate (PEDOT:PSS) is a hole injection layer (HIL), 4,4',4''-tri(carbazol-9-yl)triphenylamine (TCTA) and 1,3,5-tri(1-phenyl-1H-benzo[d]imidazol-2-yl)phenyl (TPBi) are hole transport layer (HTL) and electron transport layer (ETL), respectively, CsF is cesium fluoride as a buffer layer, and Al is aluminum as a cathode. By adjusting the mass ratio of TCTA and molecule **1** in the emitting layer (EML) from 1:1 to 1:9, the EQEs of the OLEDs were decreased from 0.25% to 0.15%. Which is mainly ascribed to the deterioration of charge mobility of the EML due to the higher concentration of molecule **1**. In addition, the two devices emitted green electroluminescent (EL) spectra predominantly located in the range of 510 and 520 nm. The outcome underscores the successful incorporation of the Br atom to obtain RTP molecules. In addition, through simultaneous modification of bromine, aromatic carbonyl, and spiroannulated phenyl moieties, fluorene-based organic phosphor molecule **3** (Figure 3) with an efficient SOC effect was designed and constructed, conferring an effective ISC process.⁶⁵ Bright green RTP emission was achieved in molecule **3**-doped isotactic poly (methyl methacrylate) film, showing a photoluminescence quantum yield (PLQY) of 21.2% and a lifetime of 5.28 ms. By using molecule **3** as the emissive material and 2,8-bis(diphenylphosphoryl)dibenzo-[b,d]thiophene (PPT) as the rigid host, the OLEDs exhibited a maximum EQE of 2.5%. Frustratingly, the device has a significant efficiency roll-off due to the long triplet lifetime of molecule **3**.

Recently, Lee et al. also reported RTP OLEDs constructed with Br-containing RTP emitter **4** (Figure 3) and a host material of 6,11-dibromodibenzo[f,h]quinoxaline (27QNX).⁶⁶ Molecule **4** exhibited yellow RTP emission peaking at 588 nm with a lifetime of 0.68 ms and PLQY of 12.3% appeared at room temperature in molecule **4**-doped 27QNX film. By further doping **4**:27QNX into TPBi host, an increased PLQY of 13.1% and a slightly short lifetime of 0.65 ms were achieved. The RTP OLEDs using molecule **4**:27QNX:TPBi as the EML exhibited a low maximum EQE

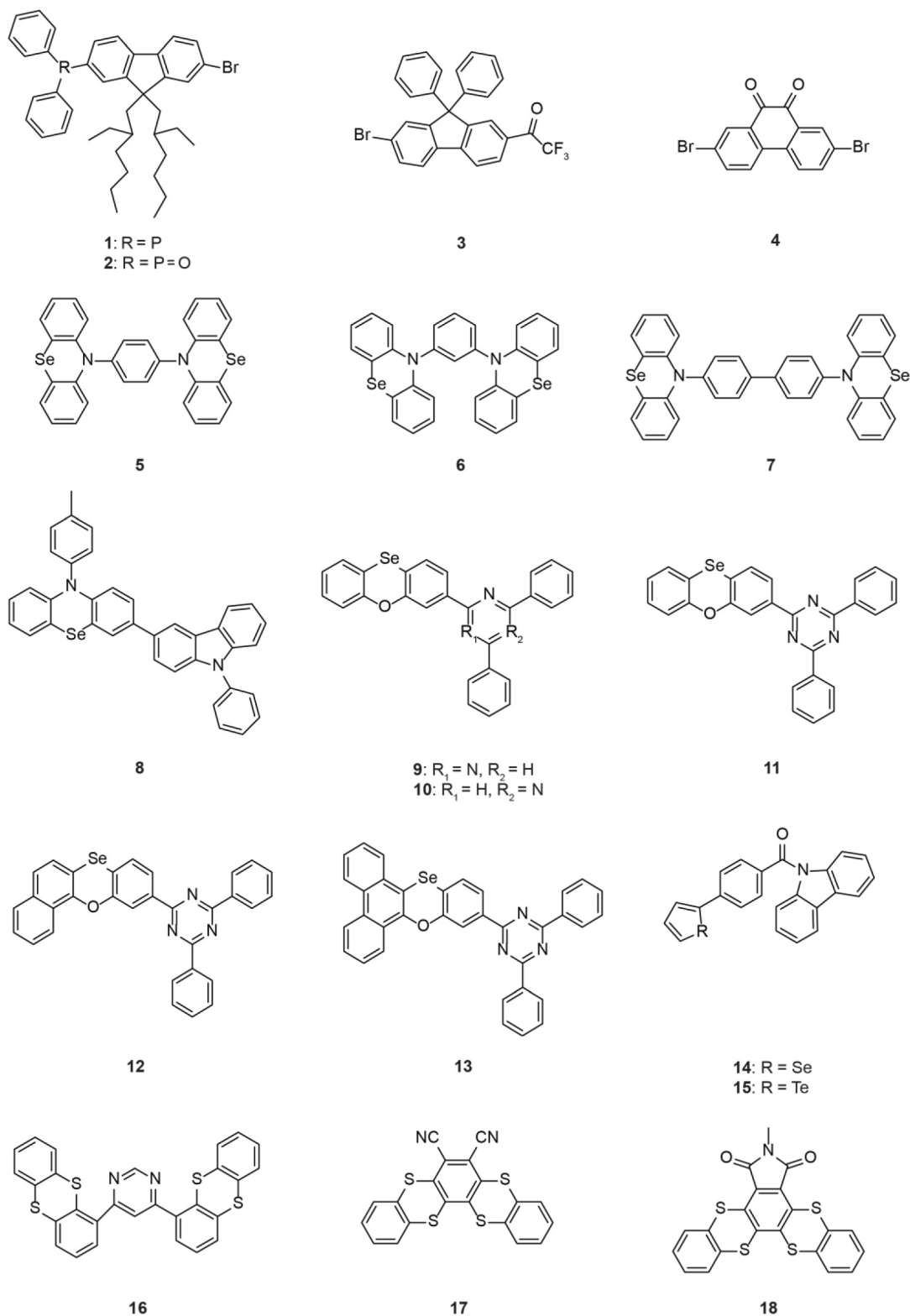


FIGURE 3 Molecular structures of 1–18.

of 0.11%, a luminance of 22.4 cd/m², and yellow emission centered at 583 nm, which places more stringent demands on further optimization of the device structure and development of the emitter to improve the performance.

Se and Br are both effective in enhancing SOC due to their heavy atom effects. However, unlike Br atom, which primarily acts as a substituent, Se can be integrated into the core molecular skeleton. This incorporation

TABLE 1 Physical properties and electroluminescence performance of RTP OLEDs.

Molecule	λ_{PL} [nm]	Φ_p [%]	τ_p [ms]	λ_{EL} [nm]	V_{on} [V]	$L_{max}/CE_{max}/PE_{max}$ [cd m ⁻² /cd A ⁻¹ /lm W ⁻¹]	EQE _{max} [%]	Refs.
1	509	-	644	510	10.5	574/-/-	0.25	45
2	516	-	1	-	-	-	-	45
3	-	21.2	5.28	-	-	1430/-/-	2.5	65
4	588	12.3	0.68	583	-	22.4/-/-	0.11	66
5	~500	33	0.61	~500	-	-	10.7	67
6	~500	35	0.64	~500	-	-	10.0	67
7	~500	27	0.93	~500	-	-	8.1	67
8	523	50.2	0.82	540	4.2	762/45.9/-	13.2	50
9	~550	38.2	1.21	~550	3.2	342.1/23.6/23.2	7.3	51
10	~550	64.0	1.24	~550	3.4	598.4/50.6/46.7	16.0	51
11	~550	68.1	0.85	~550	3.6	687.4/58.7/53.3	19.5	51
12	555	66.3	2.33	555	3.6	541.2/53.7/48.2	17.2	68
13	567	66.9	1.84	567	3.4	394.4/46.7/40.2	17.9	68
14	590	3.89	113.1	590	9.0	148.9/0.28/0.07	0.22	69
15	650	1.46	12.2	610	7.4	305.2/0.38/0.11	0.25	69
16	528	33.5	0.3	3.0	3.0	1812/23.41/24.52	7.98	70
17	597	37.0	15.2	590	3.0	-/85.5/89.9	25.1	71
18	603	68.0	12.9	-	2.8	-/43.6/52.7	18.9	71
19	466/570	-	73.9/17.4	465	3.9	1387/2.74/2.20	1.69	72
20	430/540	-	-	430/540	4.0	925/-/-	0.6	73
21	540	-	-	-	-	-	-	74
22	543	-	-	427	-	1700/	0.6	74
23	-	-	-	587-625	2.7	28,642/-/-	16	75
24	548	41.3	-	560	-	22,561/-/-	4.06	76
25	527	12.2	0.0038	-	-	51,100/-/-	7.4	77
26	536	9.4	0.0023	-	-	-	-	77
27	553	51.8	0.00054	-	-	-	-	77

TABLE 1 (Continued)

Molecule	λ_{PL} [nm]	Φ_p [%]	τ_p [ms]	λ_{EL} [nm]	V_{on} [V]	$I_{max}/CE_{max}/PE_{max}$ [cd m ⁻² /cd A ⁻¹ /lm W ⁻¹]	EQE _{max} [%]	Refs.
28	541	22.2	0.00048	-	-	-	6.85	77
29	533	17.1	0.00026	-	-	-	-	77
30	-	-	-	-	4.0	-	16.9	78
31	560	-	-	510/560	-	-	5.7	79
32	477	51	1.85	461	4.7	1000/4.0/1.8	2.6	80
33	-	-	5.5	560/690	-	-	0.000254	81
34	-	-	7.1	630/760	-	-	0.0000558	81
35	580	38	0.087	570	-	-/33.8/32.6	11.5	55
35	-	-	-	560	2.8	33,820/47.8/53.6	15.3	48
36	515	4.1	610	515	-	-	1	82
37	538	7.8	414	544	5.8	450/-/-	1.47	83
38	588	2.6	293.7	-	-	-	-	84
39	480/585	2.7	96.8/343.3	-	-	-	-	84
40	528	18	82.6	528	4.3	5167/-/-	3.3	84
41	513	80	0.003	535/485	5	-	-	44
42	505	64	0.0048	-	3.3	3295/13.4/10.5	5.8	49
43	510	55	0.00314	-	3.2	4019/4.8/3.5	2.0	49
44	510	36	0.00181	-	4.5	2123/2.8/1.2	1.6	49
45	~570	-	-	~590	-	-	0.7	85
46	~570	-	-	~590	-	-	1.6	85
47	680	0.42	1.81	680	3.6	-/3.18/-	1.59	86
48	540	84.9	-	-	3.0	17,020/49.22/53.32	14.7	52
49	496	12.2	0.00141	464	-	194/-/-	-	47
50	486	21.4	-	495	3.7	-/24.0/18.9	9.7	87

Abbreviations: EQE, external quantum efficiency; OLED, organic light-emitting diodes; RTP, room temperature phosphorescence.

significantly strengthens SOC, thus increasing the RTP emission. Lee et al. designed three metal-free RTP molecules **5–7** (Figure 3) with the introduction of Se atoms to enhance SOC.⁶⁷ The molecules **5–7**-doped bis[2-(diphenylphosphino)phenyl] ether oxide (DPEPO) films showed a broad emission at about 500 nm. The lifetime and PLQY were measured to be 610 μ s, 641 μ s, and 930 μ s as well as 33%, 35%, and 27% for molecules **5–7**-doped DPEPO films, respectively, suggesting their good RTP properties. The device utilizing emitter molecule **5** endowed a maximum EQE of 10.7%, attributed to the high PLQY of the amorphous film. Based on the same design strategy, the same group developed an RTP molecule molecule **8** (Figure 3) to enhance the radiative transition by extending the phenoselenazine core with a secondary chromophore.⁵⁰ The RTP emission at 523 nm with a remarkable PLQY of 50.2% and lifetime of 820 μ s was achieved. The high PLQY of molecule **8** enabled the excellent RTP OLED performance, showing a maximum luminance of 762 cd/m², EQE of 13.2% and CE of 45.9 cd/A.

In 2023, Su and coworkers synthesized three compounds **9–11** (Figure 3) known for their exceptional RTP feature, due to the strategic incorporation of phenoxselenine donors within donor-acceptor (D-A) architectures, which results in increased SOC for the facilitated ISC process, showing efficiencies of up to 99.2%.⁵¹ Molecules **9–11** doped 1,3-bis(N-carbazoyl)benzene (mCP) films enabled efficient RTP emissions at 550 nm with prominent PLQYs of 38.2%, 64.0%, and 68.1% and lifetime of 0.85 ms, 1.24 ms, and 1.21 ms, respectively. These compounds were utilized as emitters in a device structure comprising ITO/MoO₃/1,1-Bis[(di-4-tolylamino)phenyl]cyclohexane (TAPC)/mCP/mCP:**9–11**/1,3,5-tri(m-pyrid-3-yl-phenyl)benzene (TmPyPB)/LiF/Al (Figure 4), resulting in an EL emission at 550 nm and maximum EQEs of 16.0%, 19.5%, and 7.3%, respectively. In 2024, the same team developed two orange RTP emitters **12** and **13** (Figure 3) by using π -extended conjugation of phenoxselenine as D.⁶⁸ Doping molecule **12** or **13** into polymethyl methacrylate (PMMA) films at doping concentration of 6 wt% produces long-lived emissions at ~555 and 567 nm with lifetimes of 2.33 and 1.84 ms respectively. The PLQYs of molecules **12** and **13** were measured to be 66.3% and 66.9%, respectively. Benefitting from their excellent photophysical properties, molecules **12** and **13**-based RTP OLEDs achieved excellent maximum EQEs of 17.2% and 17.9%, CE of 53.7 cd/A and 46.7 cd/A and power efficiency (PE) of 48.2 lm/W and 40.2 lm/W at doping concentrations of 4 and 6 wt% with the device structure of ITO/TAPC/mCP/emitter:CBP/TmPyPB/LiF/Al, and the RTP OLEDs also exhibited stable and pure electrophosphorescence spectra over a wide range of driving voltages.

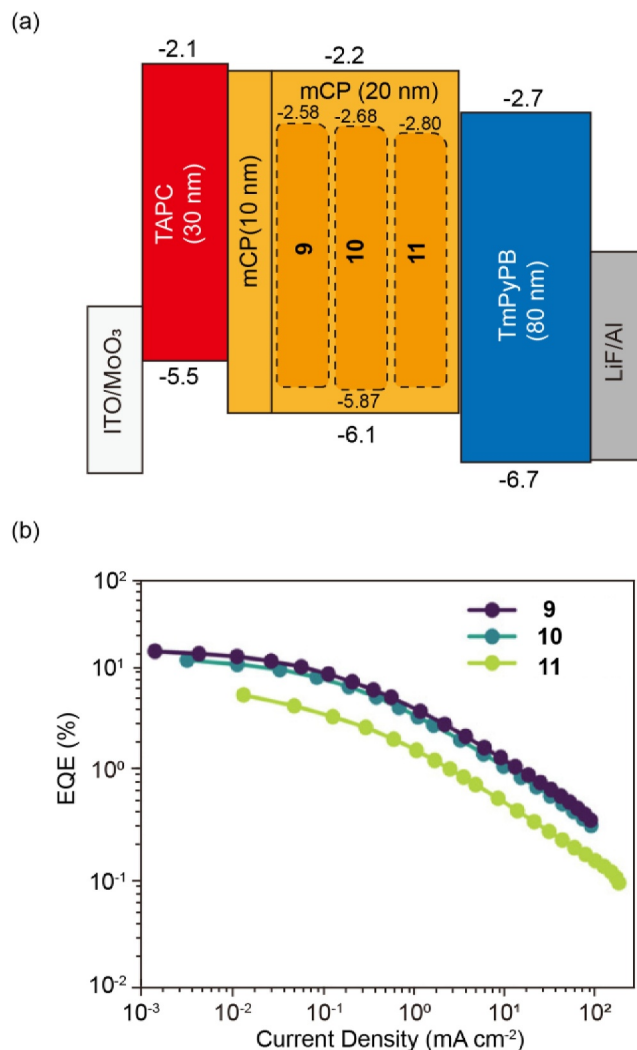


FIGURE 4 (A) Energy-level diagram, architecture, and (B) EQE-current density curves of the OLED devices using molecule **9–11** as emitters. Reproduced with permission.⁵¹ Copyright 2023, Wiley-VCH. EQE, external quantum efficiency; OLED, organic light-emitting diodes.

Huang et al. recently reported the first instance of metal-free single-molecule white emission capable of dual fluorescence and RTP emission through the introduction of chromophores of selenophene molecule **14** and tellurophene molecule **15** (Figure 3) for the enhancement of RTP emission due to the heavy atom effects of Se and tellurium (Te).⁶⁹ Specifically, compared to molecule **15** with RTP dominated emission, molecule **14** exhibited white EL via the harvest of both singlet and triplet excitons, demonstrating a Commission Internationale de l'Éclairage (CIE) coordinate of (0.30, 0.29) at 4 V, a brightness of 148.9 cd/m², a maximum EQE of 0.22%, a current efficiency (CE) of 0.28 cd/A, and a PE of 0.07 lm/W. This indicates that chalcogen atom variation could be a method for tuning the ratio of fluorescence and RTP, providing a new pathway to develop white OLEDs.

In addition to Se and Te, sulfur has been identified as an effective heavy atom to enhance SOC. An interesting study by Su et al. constructed a new organic compound molecule **16** (Figure 3) leveraging the unique properties of twisted thianthrene and pyrimidine.⁷⁰ The integration of heavy atomic sulfur and nitrogen with $n-\pi^*$ transition characteristics plays a crucial role in significantly boosting the SOC effect. This enhancement facilitated quick ISC and RTP emission, achieving impressive ISC rates of up to $1.1 \times 10^3 \text{ s}^{-1}$ and the emission peak at 528 nm with a lifetime of 304.76 μs in undoped films. Given the rapid RTP emission from amorphous films, the undoped RTP OLED using molecule **16** as EML showcased remarkable efficiency, including a turn-on voltage of 3.0 V, a maximum brightness of 1812 cd/m^2 , and a maximum EQE of 7.98%. To further enhance EQE, the same group synthesized molecules **17** and **18** (Figure 3). These molecules were designed to exhibit efficient dual emission-combining thermally activated delayed fluorescence (TADF) and RTP by incorporating sulfur atoms into the isomeric structures of pentaphene and pentacene.⁷¹ Molecules **17** and **18**, in particular, demonstrated TADF emissions at 520 and 541 nm and RTP emission bands at 597 and 603 nm, respectively. Their dual TADF and RTP capabilities resulted in high PLQYs of 37.0% and 68.0%, respectively. RTP OLEDs utilizing molecules **17** and **18** as emissive materials achieved maximum EQEs, CEs, and PEs of 8.7%, 19.3 cd/A , 21.5 lm/W , and 18.9%, 43.6 cd/A , 52.7 lm/W , respectively. These exceptional results reveal the significant potential of sulfur-bridged frameworks in advancing OLED technology. The above examples reveal that the introduction of heavy atoms is an important strategy for enhancing SOC, thus enabling increased ISC and RTP emissions in pure organic materials. Therefore, it becomes particularly critical to explore additional molecular design strategies to develop efficient RTP materials. Moreover, although the radiative rate of RTP materials is relatively fast, the excited state lifetime remains too long, and the efficiency of RTP OLEDs is still low, accompanied by severe efficiency roll-off. This also underscores the need for new device structures and material designs to further improve the performance of RTP OLEDs.

3.1.2 | Narrowed energy gap

Narrowed ΔE_{ST} can also accelerate the ISC process. It should be noted that the ΔE_{ST} can be carefully regulated through molecular engineering to suppress the reversed ISC (RISC) process, thus accelerating the k_{ISC} with moderate k_{RISC} . To limit the RISC process, ΔE_{ST} needs to be theoretically higher than 0.4 eV. In turn, by appropriately controlling the ΔE_{ST} , it is possible to switch the TADF

molecule to the RTP molecule. Therefore, RTP and TADF can coexist in many D-A type organic materials. Recently, by introducing the benzophenone as the A and the *N*-phenyl-2-naphthylamine as the donor (D), Huang et al. designed and synthesized a pure organic D- π -A- π -D compound molecule **19** (Figure 5), showing RTP properties with emission bands at 466 and 570 nm and a long lifetime of 73.9 and 17.4 ms in the solid state.⁷² The non-doped devices with the structure of ITO/MoO₃/mCP/molecule **19**/TmTyPB/LiF/Al exhibited a near white emission by utilizing the fluorescence and RTP properties, achieving maximum CE, PE, and EQE of 2.29 cd/A , 1.37 lm/W , and 1.09% and a CIE coordinate of (0.23, 0.32). The emission at 563 nm in the EL spectrum could be attributed to the radiative transition from T₁ to S₀. Furthermore, non-doped device architectures may be particularly suitable for leveraging the advantages of RTP materials. These architectures not only can effectively utilize the unique photo-physical properties of RTP materials but also can simply optimize the device fabrication procedure.

A new strategy for implementing WOLEDs was presented by the modulation of the emission color through the alteration of the molecular configuration. In 2018, a D-A molecule **20** (Figure 5), consisting of carbazole and dibenzofuran, was reported by Yamamoto's group. Molecule **20** exhibited a change in luminescent colors from near ultraviolet (350–390 nm) to white (350–650 nm) under continuous ultraviolet irradiation.⁷³ White light emission was enabled because the additional dual RTP emissions from the amorphous and crystalline states gradually emerged upon the irradiation of UV light. Interestingly, a smaller ΔE_{ST} for **20** was achieved due to the appearance of the amorphous RTP showing a slightly higher triplet energy level after photo-irradiation molecule **20**, which could be served as a bridge triplet state to decrease ΔE_{ST} . Therefore, an enhanced ISC from 7.0×10^7 to $2.0 \times 10^8 \text{ s}^{-1}$ was achieved in photo-irradiated molecule **20**. The RTP OLEDs displayed white emission with a minimum applied voltage of 4 V, a maximum luminance of 925 cd/m^2 and an EQE of 0.6%.

Phenothiazine has been extensively utilized in the development of organic luminescent materials capable of exhibiting both TADF and RTP emissions. This dual emission capability should be attributed to the presence of two distinct molecular conformers of phenothiazine, including quasi-axial (ax) and quasi-equatorial (eq) configurations, which arise from its relative flexibility that permits the tilting of the benzene rings located between the sulfur and nitrogen atoms toward each other, facilitating these unique luminescent properties. Martin et al. prepared RTP materials **21** and **22** (Figure 5) using aromatic carbonyl as A and phenothiazine as D.⁷⁴ Because of the simultaneous interaction of $n-\pi^*$ transition favored by

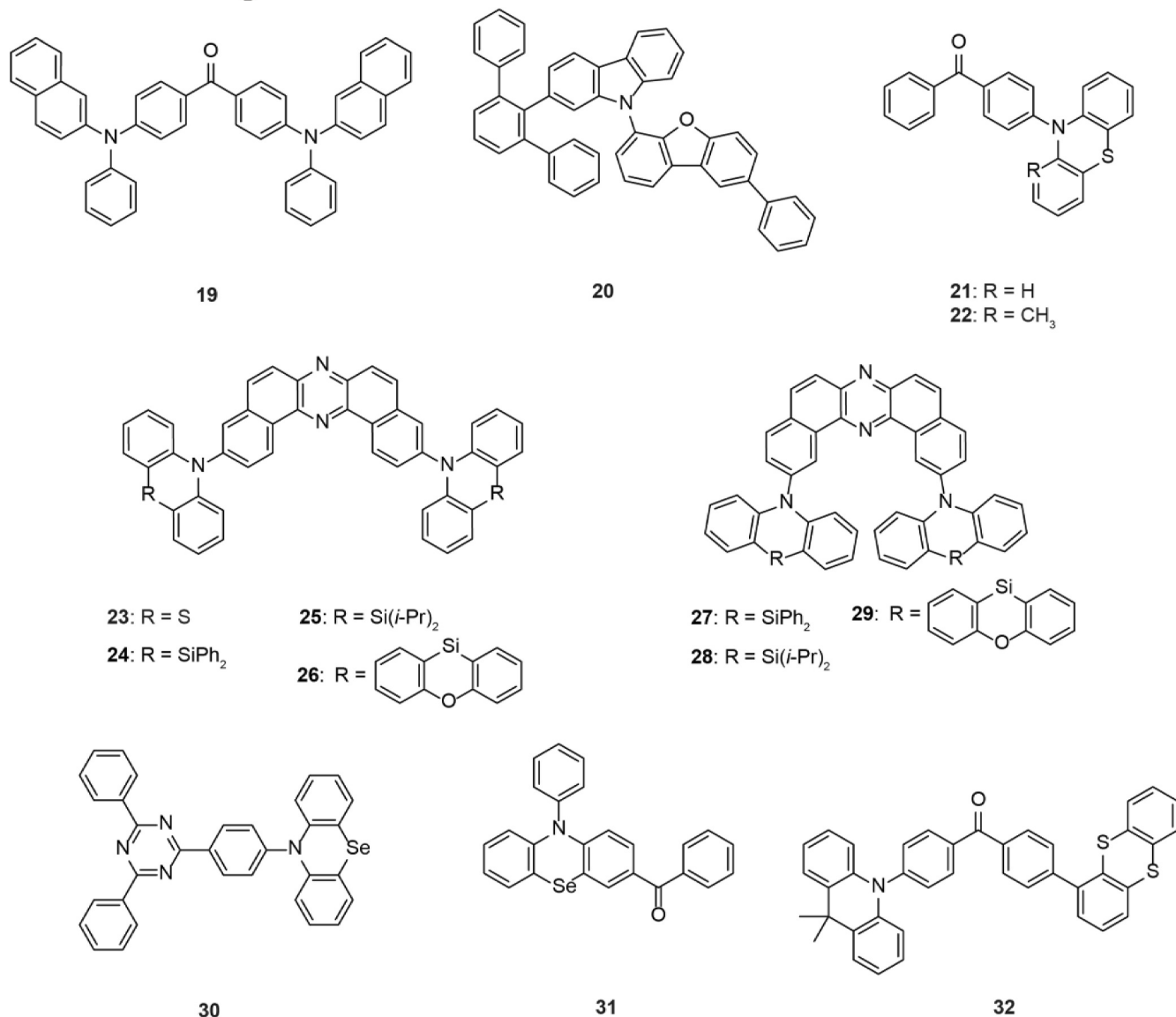


FIGURE 5 Molecular structures of **19–32**.

the carbonyl group and small ΔE_{ST} promoted by intramolecular CT (ICT), enhanced ISC process was boosted. Thus, an RTP emission was found in **21**. Moreover, through the introduction of methyl group into phenothiazine to maintain the ax conformer, planar ICT with slightly overlapped highest occupied molecular orbital (HOMO) and lowest unoccupied molecular orbital (LUMO) was achieved to keep suitable ΔE_{ST} for suppressing the RISC. Molecules **21** and **22** exhibited a RTP emission at ~ 540 nm. RTP OLED was fabricated using mCP and 10 wt% molecule **22** as the EML, showing a dual emission and a maximum EQE of only 0.6%.

In 2019, a heavy-atom-free D-A-D emitter **23** (Figure 5) using dibenzo[*a,j*]phenazine as A unit and phenothiazine as D unit was reported by Data, in which the distinct emission paths for TADF and RTP can be achieved through controlling the molecular conformations in various

polarities solvent for tuning the ΔE_{ST} (Figure 6A).⁷⁵ When molecule **23** was in ax-ax configuration, RTP emission dominated the luminescent process; when molecule **23** was in eq-eq and ax-eq conformers, a much-separated HOMO and LUMO distributions than that of ax-ax conformer was empowered, thus resulting in a small ΔE_{ST} and leading to the TADF dominated emission process. Through tuning the deposition solvents for controlling the conformers, tunable EL spectra spanning from 587 to 625 nm were achieved in the OLEDs when using molecule **23** as emitters, which enabled a significant advancement in the development of OLED devices with tunable emission colors and efficiencies. With the same design strategy, the same group developed a new D-A-D type TADF/RTP hybrid emitter molecule **24** (Figure 5) using dihydrophenazasiline as D and phenothiazine as A.⁷⁶ These results suggest that by carefully selecting the

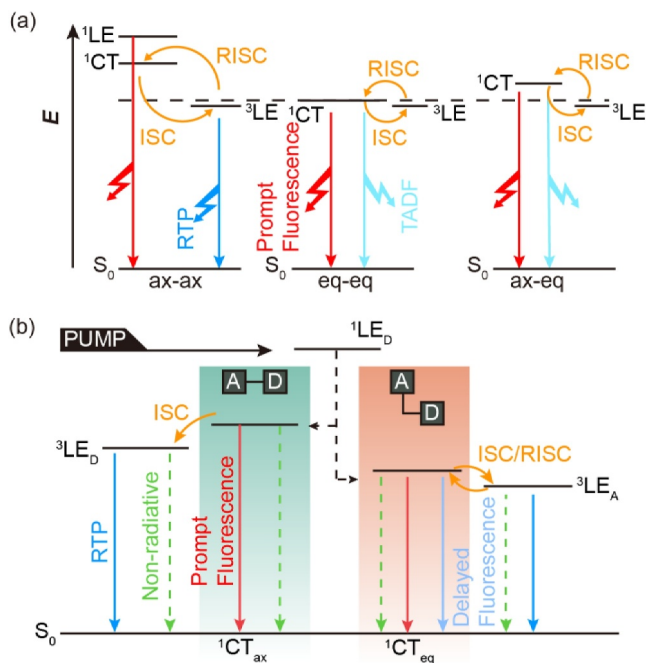


FIGURE 6 Energy diagram of the photophysical processes of (A) molecule **23**. Reproduced with permission.⁷⁵ Copyright 2019, Royal Society of Chemistry. (B) Molecule **30** in different conformers. Reproduced with permission.⁷⁸ Copyright 2019, Royal Society of Chemistry.

host matrix, the energies of the singlet and triplet excited states for molecule **24** could be precisely modulated, thereby allowing for the regulation of emission properties between TADF and RTP. The polarity host of DPEPO could greatly decrease the excited charge transfer singlet state (^1CT) but had limited influence on the locally excited triplet state (^3LE), thus leading to the narrowed ΔE_{ST} for enabling TADF dominated emission peaked at 482.5 nm. In addition, pure RTP emission peaked at ~548 nm with a PLQY of 41.3% was achieved in TCTA matrix. The RTP OLED was fabricated using ITO/NPB/TAPC/10 wt% molecule **24**:TCTA/TPBi/LiF/Al. *N,N'*-Bis(naphthalen-1-yl)-*N,N'*-bis(phenyl)benzidine (NPB) and TAPC are the HIL and HTL in the device. The OLED reached an EQE of 4.06% and a brightness of 22 561 cd/m². Moreover, to investigate how substituents on the silicon atom and the regioisomerism of compound molecule **24** influence the photophysical properties, the same group synthesized a range of D-A-D structure molecules **25–29** (Figure 5).⁷⁷ It appears that a smaller substituent on the silicon center facilitated vibrational interaction between the D and A parts, enhancing TADF. Conversely, for the RTP process to be favored, molecular motion needed to be minimized. Therefore, the presence of larger substituents on the silicon center resulted in a more pronounced RTP. Thus, the PLQYs improved with the increase in size of the substituents of molecules **25–29**. Specially, when doped these molecules into TCTA host, RTP emission was found,

showing emission peaks at 527 nm, 536 nm, 553 nm, 541 nm, and 533 nm, lifetimes of 3.8, 2.3, 0.54, 0.48, and 0.26 μs , and PLQYs of 12.2%, 9.4%, 51.8%, 22.2%, and 17.1% for molecules **25–29**, respectively. RTP OLEDs utilizing compounds **25** and **28** achieved EQEs of 7.4% and 6.85%, respectively.

Phenoselenazine, which is similar to phenothiazine and phenazasiline, features two conformers of ax and eq that can influence the TADF and RTP emission pathways. Molecule **30** was synthesized by Lee et al. using phenoselenazine as D and 1,3,5-triphenyl-2,4,6-triazine as A.⁷⁸ Because of the difference in conformation and the heavy atomic effect of Se atoms, molecule **30** exhibited two distinct relaxation dynamics of TADF and RTP via tuning the singlet and triplet energy level. The ax conformer is more planar, leading to a higher mixed CT/local excited (LE) character, which enabled a rapid ISC from the singlet charge transfer state (CT_{ax}) to the low lying local excited triplet state of D ($^3\text{LE}_{\text{D}}$), conferring the RTP emission from the D unit. On the other hand, the eq conformer is more orthogonal, which resulted in more decoupled HOMO and LUMO distributions for a lower CT state and a smaller energy gap with the local excited triplet state of the A ($^3\text{LE}_{\text{A}}$), thereby facilitating TADF through ISC and RISC (Figure 6B). A maximum EQE of 16.9% was achieved in an optimized OLEDs using molecule **30** as emissive material. It should be noted that the high device performance should originate from the TADF emission process. Recently, the same group also constructed molecule **31** (Figure 5) which consists of a phenoselenazine core decorated with a benzoyl functional group, both green TADF and yellow RTP emissions were observed in molecule **31**.⁷⁹ The two unique emissions were produced by its two conformers. For the conformer with orthogonal orientation between *N*-phenyl fragment and phenoselenazine moiety, a significant overlap between the HOMO and LUMO leads to a relatively large ΔE_{ST} making RISC unlikely; with the aid of the heavy atom effect of Se, RTP emission became the predominant emission process. In contrast, for the conformer with a parallel fashion between *N*-phenyl fragment and phenoselenazine moiety, a greater spatial separation between the HOMO and LUMO was achieved, which resulted in a decreased ΔE_{ST} , thus enabling TADF dominated emission process. Molecule **31** demonstrated a TADF emission at 510 nm and RTP emission at 560 nm. The OLEDs with the structure of ITO/PEDOT:PSS/TAPC/mCP/DPEPO:molecule **31**/diphenyl[4-(triphenylsilyl)phenyl]phosphine oxide (TSPO1)/TPBi/LiF/Al were fabricated at doping concentrations of 10 wt%, 20 wt%, 30 wt%, and 40 wt%. The EQE was up to 5.7% at 20 wt% doping concentrations of molecule **31**. Interestingly, the EL spectra evolved with variations in applied voltage and doping levels, displaying two distinct emission peaks at 510 and 560 nm (Figure 7).

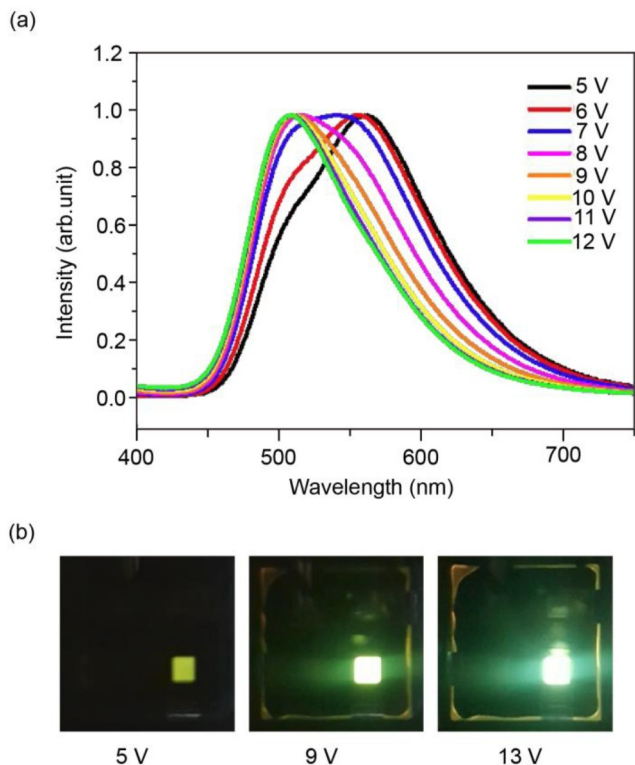


FIGURE 7 (A) Voltage-dependent EL spectra and (B) photographs of the RTP OLEDs using molecule **31** as EML. Reproduced with permission.⁷⁹ Copyright 2020, American Chemical Society. EML, emitting layer; OLED, organic light-emitting diodes; RTP, room temperature phosphorescence.

These observations support the notion that the peaks were attributable to TADF and RTP, respectively, which indicates that the relative intensity of the two emission components could be controlled by current density.

In 2019, Grazulevicius designed an asymmetric D-A-D' molecule **32** (Figure 5), which adopted diphenylsulfone as A, and acridan and thianthrene as donors, respectively.⁸⁰ Due to the concurrent influence of the $n-\pi^*$ transition induced by the sulfone group, and the minimal ΔE_{ST} encouraged by ICT, an augmentation of the ISC process was conferred, thus rendering molecule **32** as an RTP emitter with an emission peak at 477 nm, PLQY of 51%, and a lifetime of 1.85 ms. When doped in DPEPO, molecule **32** discovered inefficient TADF and obvious RTP emissions. The OLED using molecule **32** as RTP emitters endowed a maximum EQE of 2.6%.

3.2 | Reduced triplet exciton deactivation

Since pure organic materials exhibit a small radiative decay rate of triplet excitons, reducing triplet exciton deactivation through minimizing the $k_{nr} + k_q$ is crucial

for achieving efficient organic RTP emitters. In recent years, the host-guest system and molecular aggregation have been proposed to suppress the non-radiative deactivation pathways of long-lived triplet excitons.

3.2.1 | Host-guest system

In the host-guest system, the host provides a rigid environment that not only blocks the non-radiative decay channels of the guest molecules, but also avoids aggregation-induced quenching. The selection of host materials is very crucial to enhance the performance of RTP OLEDs. First, the appropriate HOMO and LUMO energy levels of the host materials play a critical role in promoting effective exciton formation. Second, the host materials should have balanced carrier mobility to broaden the recombination zone of the emitting layer. Third, the host and guest materials should have good compatibility to ensure uniform morphology and prevent phase separation for improving device stability. Finally, the triplet energy level of the host material should be higher than that of the RTP guest to optimize energy transfer for mitigating the exciton quenching.

In 2013, Chaudhuri and colleagues achieved a breakthrough by demonstrating RTP OLED, which uniquely combined fluorescence and RTP in purely organic materials. They introduced two new molecules **33** and **34** (Figure 8) through the synthesis of thienyl-decorated phenazine (molecule **33**) and its link to a triphenylene block (molecule **34**), which showed effective triplet relaxation bottlenecking due to their weak SOC effect.⁸¹ By using molecule **33** or molecule **34** doped polyvinylcarbazole (PVK) films as EML, OLEDs exhibited two EL peaks at 560 and 690 nm for molecule **33**, and at 630 and 760 nm for molecule **34**, corresponding to the fluorescence and RTP emissions, respectively. Moreover, the maximum EQEs were only 2.54×10^{-4} and 5.58×10^{-5} for molecule **33** and molecule **34**. The relatively low EQEs may be due to the low PLQYs. Despite the dominance of fluorescence in EL and the relatively low EQEs, this research paved the way for the development of RT OLEDs operable at ambient conditions.

In 2019, Wang's team developed an organic RTP material molecule **35** (Figure 8), which showed a dual fluorescence and RTP emission peaked at around 485 and 580 nm.⁴⁸ Interestingly, when molecule **35** was doped into a host material of TRZ-BIM (Figure 9) with 10 wt% doping concentrations, a significantly improved RTP property was realized, demonstrating an emission at 570 nm with a PhQY of 38% and a lifetime of 87.0 μ s. This hybrid film as EML enabled the fabrication of highly efficient RTP OLEDs with a maximum EQE of 11.5%

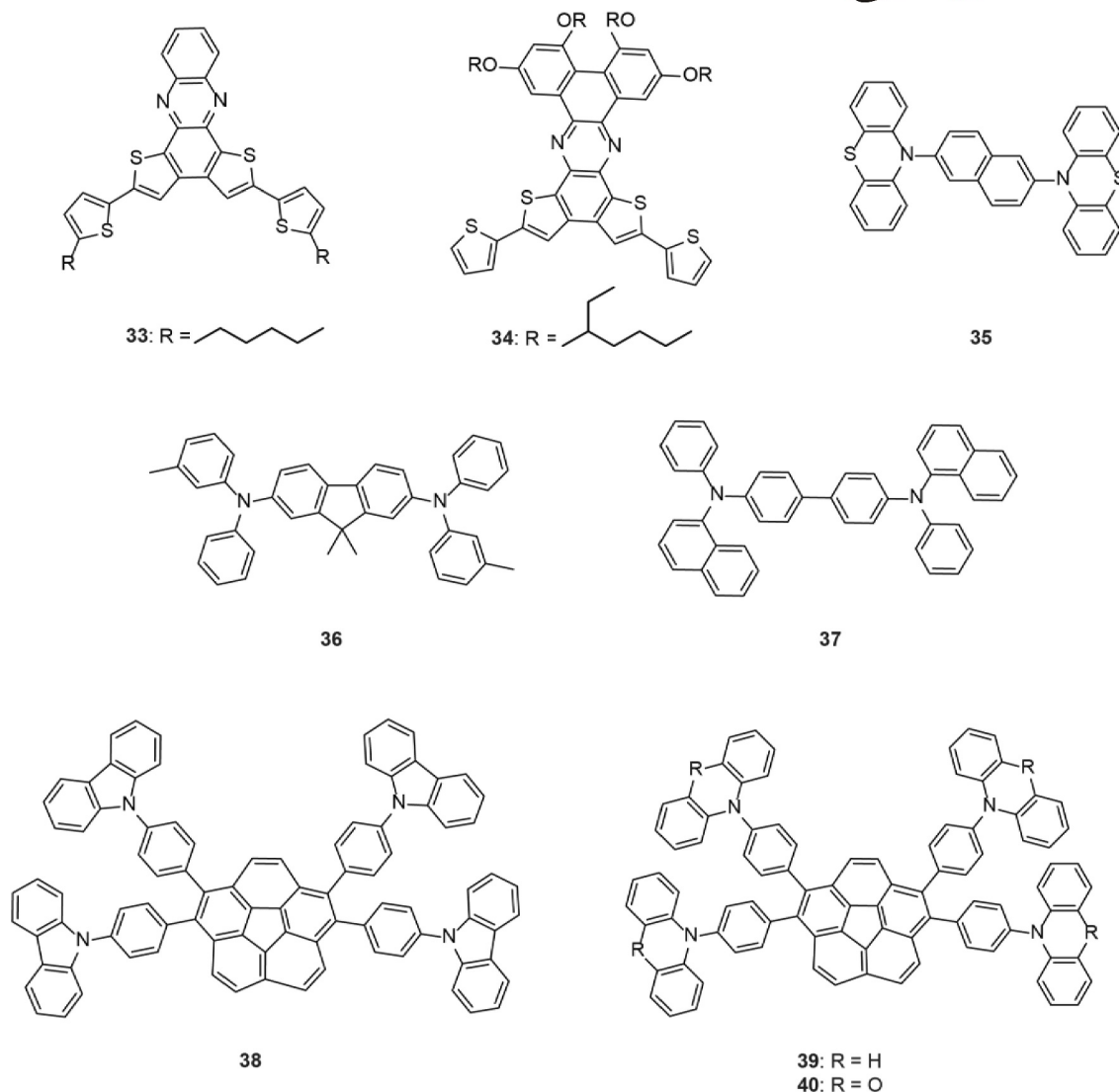


FIGURE 8 Molecular structures of 33–40.

(Figure 9), PE of 32.6 lm/W, and CE of 33.8 cd/A. Shortly, molecule 35-doped TRZ-BIM film was also employed as an RTP sensitizer to develop RTP-sensitized fluorescent devices.⁸² The device achieved a maximum EQE and CE of 15.3% and 47.8 cd/A, respectively. This innovation overcomes the limitation of low PLQYs of organic RTP materials, providing a new direction to break the 5% EQE limit of fluorescent OLED devices.

Due to the ultralong lifetime of RTP emitters, afterglow OLEDs were also developed. In 2015, Adachi et al. selected carbazole as a conductive unit and a hydrophobic steroid derivative as a stiff moiety, and a rigid RTP host molecule, 3-(*N*-carbazolyl)-androst-2-ene (CzSte) was designed.⁴⁶ By doping RTP emitter 36 (Figure 8) and its deuterated analog molecule 36-d₃₆ into the CzSte host film with a concentration of 1 wt%, dual fluorescence (400 nm) and RTP (515 nm) emissions were achieved due to the suppressed molecular vibrations and non-radiative decay of the guest

emitters induced by the intermolecular interactions of the rigid CzSte host. The green RTP emission from molecule 36-d₃₆-doped CzSte film showed an ultralong lifetime of 0.69 s and a PhQY of 4.1%. By using molecule 36-d₃₆-doped CzSte film as EML, the afterglow OLEDs were fabricated, which exhibited a special EL behavior. Under the applied voltage, a blue emission from fluorescence was observed. In contrast, the device showed an extraordinary green persistent emission from the RTP emission of molecule 36-d₃₆ when the applied voltage was removed (Figure 10), thus rendering the electrically driven RTP OLED with an afterglow emission. The lifetime was up to 0.39 s and the afterglow spectra could still be recorded with a delayed time of 0.6 s. Although the maximum EQE was only 1%, the device could endow a dual emission with fluorescence and afterglow emissions.

In 2022, Tao et al. selected the widely utilized electron-transport material PPT as the rigid host, and the

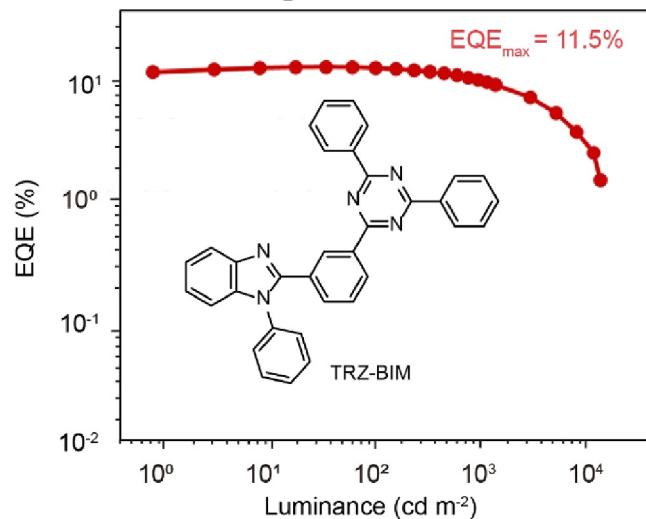


FIGURE 9 EQE of RTP OLEDs with molecule 35/TRZ-BIM as EML. The inset shows the molecular structure of TRZ-BIM. Reproduced with permission.⁴⁸ Copyright 2019, American Chemical Society. EML, emitting layer; EQE, external quantum efficiency; OLED, organic light-emitting diodes; RTP, room temperature phosphorescence.

hole-transport material NPB molecule **37** (Figure 8) as the emissive RTP dopant.⁸³ Leveraging the structurally rigid amorphous matrix provided by PPT, this approach effectively mitigated the non-radiative decay of triplet excitons of molecule **37**. Remarkably prolonged RTP emission at 540 nm with lifetimes ranging from 414 to 387 ms was achieved in the 1 wt% to 10 wt% molecule **37**-doped PPT film. The optimized afterglow OLEDs demonstrated dual fluorescence and RTP emission with a maximum EQE of 1.47%, CE of 1.01 cd/A, PE of 0.55 lm/W, and luminance of 609 cd/m² (Figure 11). In addition, the lifetime (EL) of RTP emission for molecule **37** was 356 ms, which was comparable to the corresponding lifetime of PL (Figure 11B), thus endowing an afterglow emission after turning off the driving voltages. It was observed that due to the diminished suppression of non-radiative processes with the increasing doping concentration of molecule **37**, the EL lifetimes were slightly decreased. These results highlight the effectiveness of the host-guest doping approach in developing OLEDs that offer both high operational efficiency and prolonged afterglow, significantly enhancing the application of RTP materials in next-generation OLEDs.

Si and coworkers developed a series of multi-donors modified corannulene-derived RTP emitters **38–40** (Figure 8).⁸⁴ When molecules **38–40** were doped into mCP host, multiple RTP emissions were realized. Molecule **38**-doped mCP film demonstrated RTP emission from a localized corannulene core, showing an emission peak at 588 nm with a lifetime of 293.7 ms and PhQY of

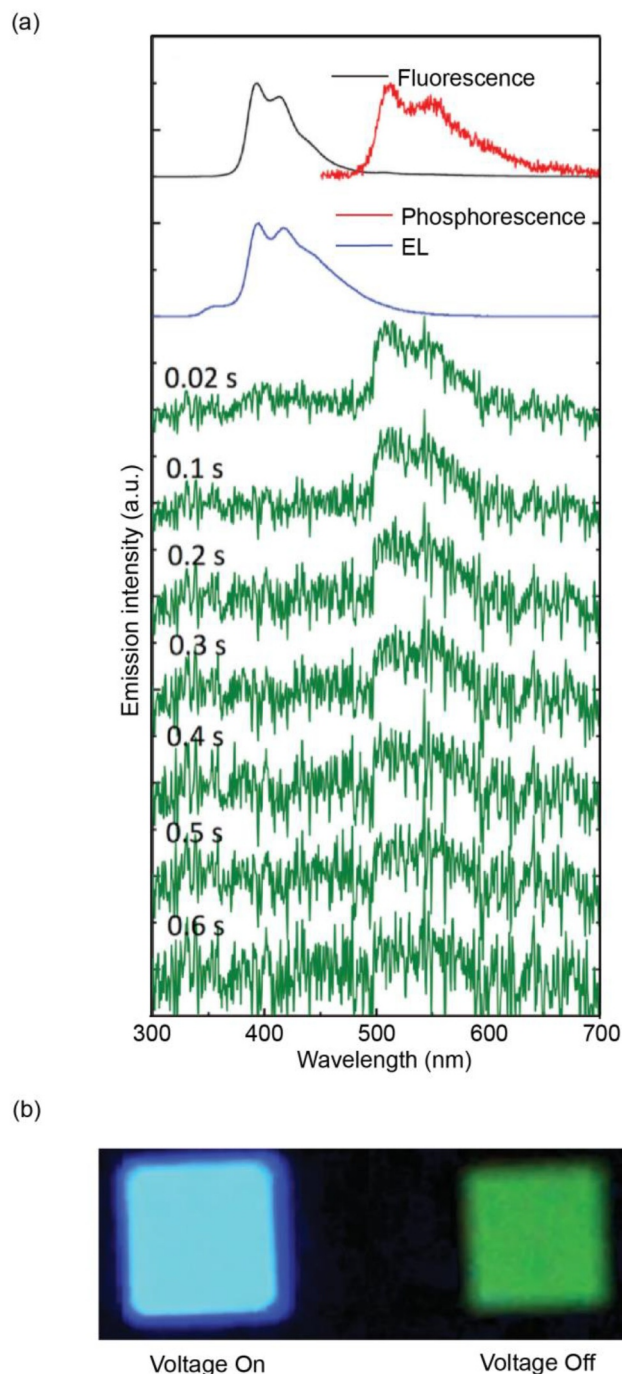


FIGURE 10 (A) Fluorescence (black) and phosphorescence (red) spectra of molecule **36**-d₃₆-doped CzSte film, and EL spectra of OLED with **36**-d₃₆-doped CzSte film as EML during (blue) and after (green) electrical excitation. (B) Photographs of EL during (left) and after (right) electrical excitation. Reproduced with permission.⁴⁶ Copyright 2015, Wiley-VCH. EL, electroluminescent; EML, emitting layer; OLED, organic light-emitting diodes.

2.6%. Molecule **39**-doped mCP film exhibited dual RTP emission attributed to both higher-lying T₁ and lower-lying T₁ states, endowing emission peaks at 480 and

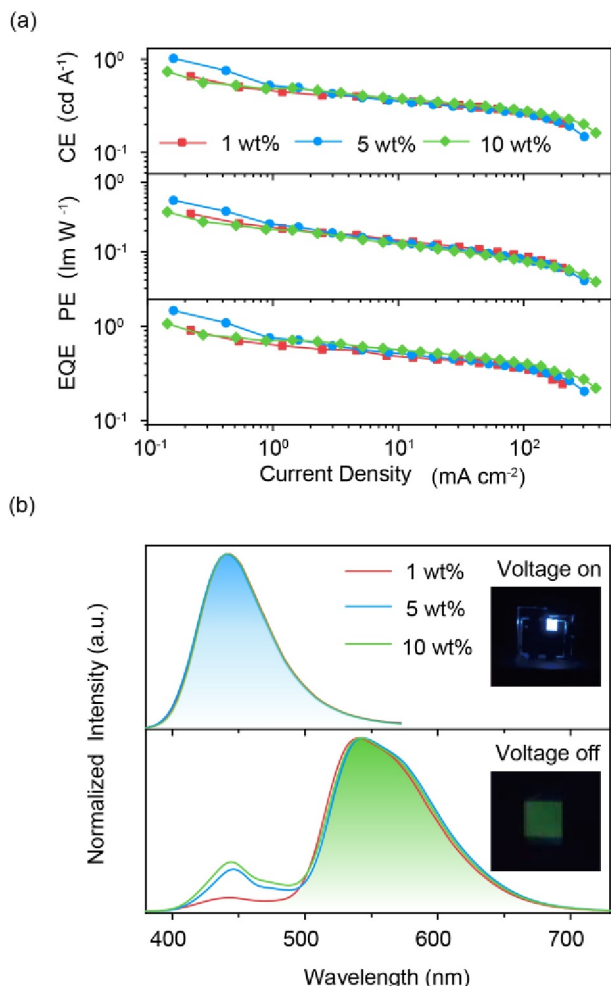


FIGURE 11 (A) Efficiencies-current density, (B) EL spectra during (top) and after (bottom) electrical excitation of the OLED using molecule **37**-doped PPT film as EML. Reproduced with permission.⁸³ Copyright 2022, AIP Publishing. EML, emitting layer; OLED, organic light-emitting diodes.

585 nm with lifetimes of 96.8 and 343.3 ms and PhQY of 2.7%, respectively. Molecule **40**-doped mCP film achieved an RTP emission originated from higher-lying T₁ states, rendering an emission peak at 528 nm with a lifetime of 82.6 ms and PhQY of 18.0%. This higher-lying T₁ involved in the emission process indeed deviated from Kasha's rule, which generally dictates emission from the lowest T₁ state. Solution-processed afterglow OLED using molecule **40**-doped mCP film as EML was constructed, and a turn-on voltage of 4.3 V with a maximum EQE of 3.3% and a luminance of 5167 cd/m² were achieved.

3.2.2 | Molecular aggregation

Molecular aggregation engineering is pivotal in developing RTP materials as it enables the precise arrangement of molecules to facilitate efficient ISC and suppresses the non-radiative decay to achieve enhanced RTP emission. By

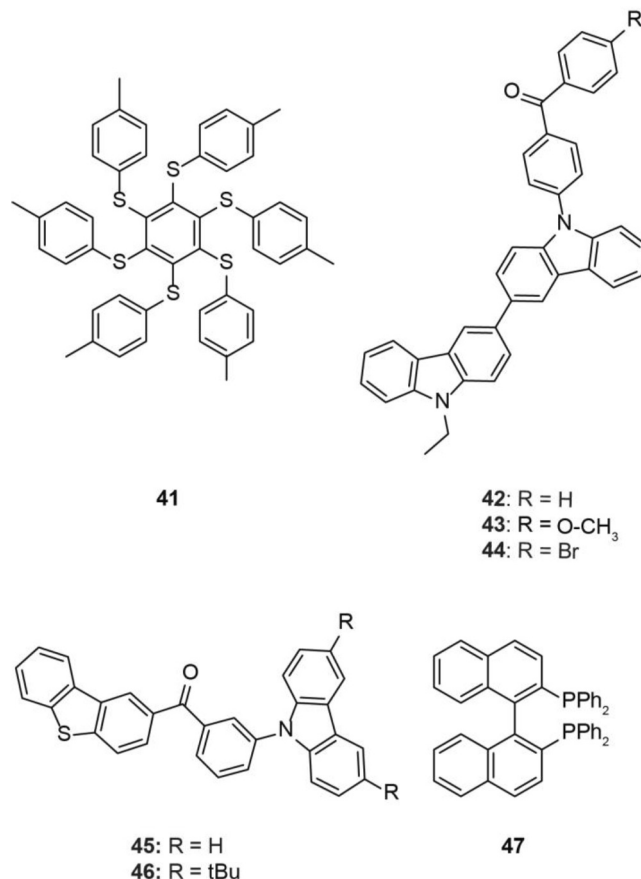


FIGURE 12 Molecular structures of **41**–**47**.

controlling molecular interactions and packing in the solid state, RTP properties including PLQY and lifetime can be rationally manipulated. In 2013, Bergamini et al. synthesized a RTP molecule **41** (Figure 12) using a hexathio-benzene core and peripheral tolyl substituents.⁴⁴ Molecule **41** showed outstanding RTP in solid state due to the restrained intramolecular rotation of C-S bond and the reduced conformational mobility of the tolylthio substituents in a rigid environment for the suppressed non-radiative decay of the triplet exciton. Molecule **41** demonstrated a green luminescence with an emission peak at 513 nm, a lifetime of 3 μs, and a PLQY of 80%. The solution-processed OLED with the device structure of ITO/PEDOT:PSS/PVK:PBD:5 wt% molecule **41**/Ba/Al was fabricated. PVK has good hole transporting properties and a high triplet energy level, which was used to be the host material to provide a rigid environment; 2-(4-biphenyl)-5-(4-tert-butylphenyl)-1,3,4-oxadiazole (PBD) was used to improve the charge balance of the EML. The devices exhibited an EL spectra peaking at 485 nm, a maximum EQE and CE of 0.1% and 0.5 cd/A at 11 V, respectively. Because of the low rigidity of the polymer host, the grievous deactivation process of triplet excitons in molecule **41** occurred, which resulted in low device performance.

In 2019, Zhang et al. prepared a series of aggregation-induced RTP molecules **42–44** (Figure 12) by integrating triplet-state enhanced moieties of carbonyl and halide substituted carbonyl into the biscarbazole unit.⁴⁹ Molecules **42–44** exhibited intense RTP luminescence, showing emission peaks of 505 nm, 510 and 510 nm, lifetimes of 4.80, 3.14 and 1.81 μ s, as well as remarkable solid-state PhQYs of 64%, 55%, and 36%, respectively. The undoped RTP OLEDs using **42** and **43** as homogeneous EMLs showed a minimum turn-on voltage of 3.2 V, a maximum luminescence of 4019 cd/m^2 , and a maximum EQE of 5.8% as well as a relatively small efficiency roll-off.

In 2020, Lee et al. reported two pure organic aggregation-induced emission materials **45** and **46** (Figure 12) through adopting asymmetric D-A-D' structures in which benzoyl served as the A segment and dibenzothiophene and carbazole derivatives served as D units, respectively.⁸⁵ Both molecules exhibited obvious dual emission in crystals, with a blue emission from intramolecular TADF at \sim 450 nm and an orange emission from intermolecular RTP emission at \sim 570 nm. This unique luminescent property was used to explore the white RTP OLEDs using non-doped devices with a configuration of ITO/TAPC/mCP/molecule **45**/tris-[3-(3-pyridyl)mesityl]borane (3TPYMB)/LiF/Al. The EL spectrum showed a dual TADF emission at \sim 464 nm and RTP emission at \sim 590 nm, rendering a white emission with a maximum EQE of \sim 0.7%. The low efficiency of the non-doped OLED should be mainly due to the long lifetime of triplet excitons.

To further investigate the influence of packing dimers on the RTP properties, Zhu and coworkers reported a type of RTP material **47** (Figure 12) with racemic molecular configuration.⁸⁶ Compared to the chiral counterpart, the racemic molecule **47** demonstrated alternative cross-packing of R- and S- forms of molecule **47** in crystals, which not only significantly inhibited the bimolecular quenching pathway and triplet-triplet annihilation (TTA) but also inhibited the non-radiative pathway of triplet excitons, thus resulting in the enhancement of the RTP intensity and much deeper red RTP emission at 680 nm with a PhQY of 0.42%, and lifetime of 18.1 ms. To probe the EL properties, an OLED was fabricated with the configuration of ITO/PEDOT:PSS/TAPC/mCP/molecule **47**/TmPyPB/CsF/Al. The device displayed a maximum EQE of 1.59%, PE of 3.03 lm/W , and CE of 3.18 cd/A . Moreover, molecule **47** showcased a more harmonized blend of fluorescence and phosphorescence compared to its chiral counterpart, thus allowing the generation of white-light emission with a color-rendering index of 73 and a commission international de L'Eclairage coordinate of (0.37, 0.44).

In 2023, Su et al. designed and produced a polycyclic aromatic hydrocarbon molecule **48** (Figure 13) featuring

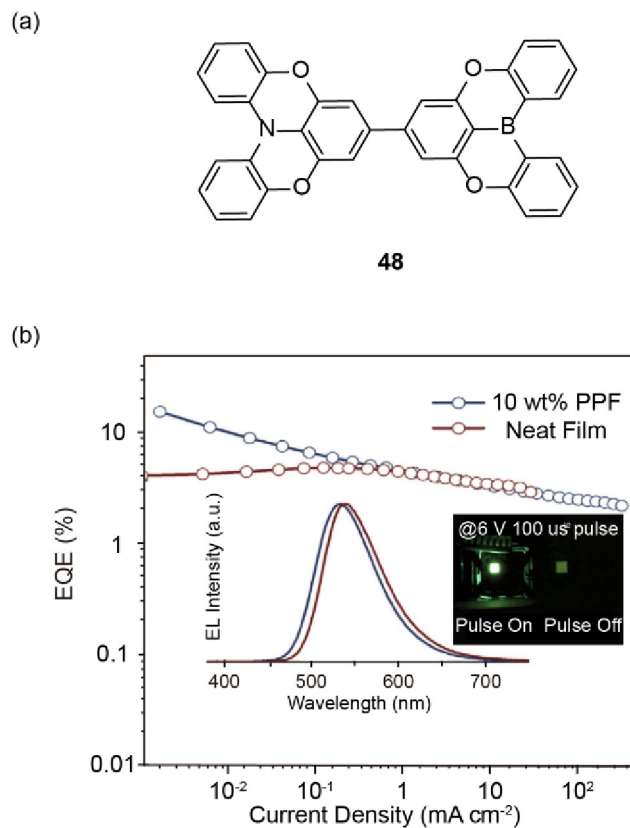


FIGURE 13 (A) Molecular structure of **48**. (B) The EQE of 10 wt % molecule **48**-doped PPF and nondoped devices. The inset showed the RTP OLED based on 10 wt % molecule **48**:PPF under the pulse voltage switch on at 6 V and off. Reproduced with permission.⁵² Copyright 2023, Elsevier. EQE, external quantum efficiency; OLED, organic light-emitting diodes; RTP, room temperature phosphorescence.

heteroatoms such as boron, nitrogen, and oxygen. These heteroatoms facilitated strong π - π interactions and J-aggregation in the dimer, enhancing the transition dipole moment in a densely stacked structure.⁵² The PL in both 10 wt% doped and pure films showed high PLQYs of 87.9% and 84.9%, respectively, due to the formation of aggregated dimers. The undoped OLED achieved a maximum EQE of 4%. In contrast, by using 2,8-bis(diphenylphosphoryl) dibenzo[b,d]furan (PPF) as the host, OLEDs achieved outstanding performance, exhibiting a maximum EQE of 14.7%, CE of 49.22 cd/A , PE of 53.32 lm/W , and luminance of 17,020 cd/m^2 , along with an afterglow emission with a lifetime of \sim 157 ms. The remarkable afterglow emission observed under electrical stimulation likely originated from the field-induced dissociation of triplet exciton followed by their recombination.

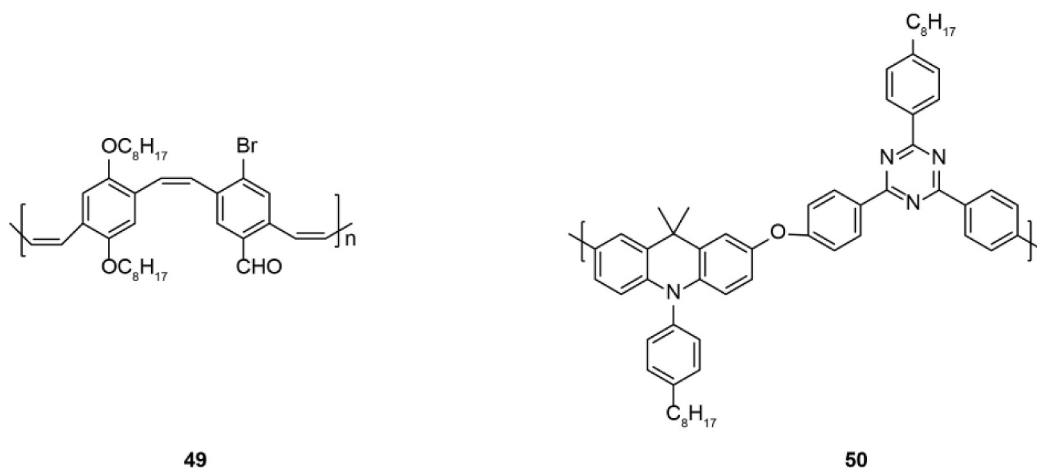
3.2.3 | Polymerization

The intertwined structure of the polymer can not only provide a rigid environment to immobilize the phosphor,

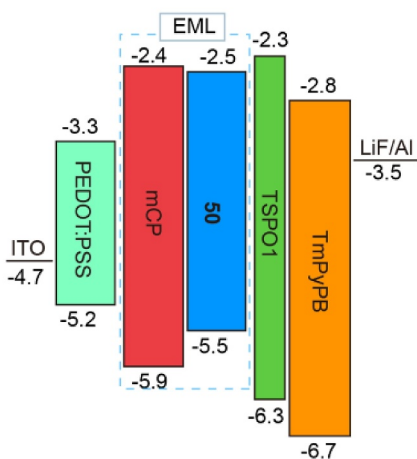
suppressing nonradiative transitions, but also isolate oxygen and humidity to avoid triplet exciton quenching. Nevertheless, the majority of polymer matrices exhibit electrical insulating properties, limiting the widespread application of RTP polymers in RTP OLEDs. In 2018, He et al. synthesized an RTP polymer molecule **49** (Figure 14A) containing bromine atoms, exhibiting a blue emission at 496 nm and a PLQY of 12.2%.⁴⁷ Benefiting from the simultaneous interactions of Br and aromatic aldehyde substituent groups, an emission lifetime of 14.1 μs was achieved, confirming its RTP property. The RTP OLED using ITO/PEDOT:PSS/PVK:PBD:0.5 wt% molecule **49**/TmPyPB/Liq/Al as the structure was fabricated, showing a maximum luminance of 194 cd/m^2 . Recently, Ding et al. Designed an RTP

polymer molecule **50** (Figure 14A) based on the D-oxygen (O)-A architecture that can be utilized for solution-processed RTP OLEDs.⁸⁷ The O atom not only acts as a spacer to reduce HOMO and LUMO orbital overlap and suppress the CT fluorescence, but also enhances the SOC to accelerate ISC, resulting in excellent RTP performance. Molecule **50** showcased a vivid sky-blue emission that peaked at 486 nm and PLQY of 21.4%. The solution-processed RTP OLED (ITO/PEDOT:PSS/mCP:15 wt% molecule **50**/TSPO1/TmPyPB/LiF/Al (Figure 14B) achieved a record-high EQE of 9.7% (Figure 14C), CE of 24.0 cd/A , and PE of 18.9 lm/W , respectively. The high EQE of the device demonstrates the enormous potential of pure organic RTP polymers in solution-processed OLEDs.

(a)



(b)



(c)

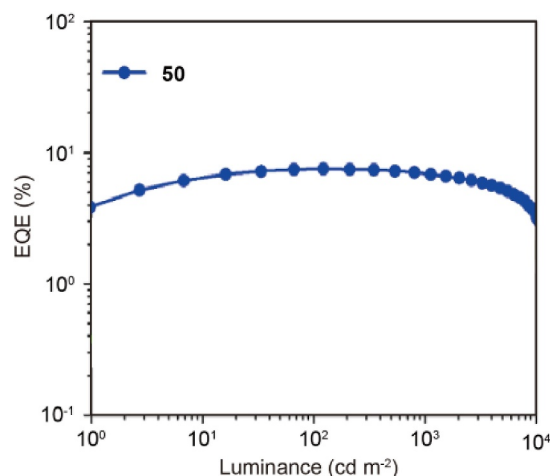


FIGURE 14 (A) Molecular structures of **49** and **50**. (B) Device structure and related energy level diagram and (c) EQE curve of OLED using molecule **50**-doped mCP films as EML. Reproduced with permission.^{47,87} Copyright 2020, Wiley-VCH. EML, emitting layer; EQE, external quantum efficiency; OLED, organic light-emitting diodes.

4 | CONCLUSION AND FUTURE PERSPECTIVES

The integration of RTP materials into OLEDs heralds a significant shift toward more sustainable and innovative optoelectronic devices. RTP materials, devoid of heavy metals, promise an eco-friendly alternative to traditional phosphorescent emitters, aligning with the growing demand for green technology. However, their application faces hurdles, primarily due to weak SOC in organic molecules, which impedes efficient phosphorescence at room temperature. Additionally, challenges such as oxygen quenching, and thermal vibrations further complicate their practical application in OLEDs. Despite these obstacles, the field of RTP materials is advancing rapidly, with research efforts concentrated on enhancing SOC through molecular design and mitigating non-radiative losses. Innovations in synthesizing RTP materials with heavy atoms such as bromine or novel organic frameworks have shown potential in overcoming the inherent limitations of organic phosphorescence. Concurrently, strategies to protect RTP materials from external quenching factors and optimize device architecture are paving the way for more efficient and durable RTP OLEDs. The potential of RTP materials extends beyond OLEDs, promising advancements in security, bio-imaging, and information storage, among others. Their unique RTP properties open new avenues for application, emphasizing the versatility and wide-ranging impact of RTP technology. As research progresses, the synthesis of new RTP materials with optimized properties is expected to address current performance gaps, heralding a new era of high-efficiency, eco-friendly OLEDs.

In conclusion, RTP materials stand at the forefront of a revolution in OLED technology, offering a path toward devices that are not only more efficient and versatile but also environmentally sustainable. While challenges remain, the relentless pursuit of innovation in molecular design and device engineering holds the promise of overcoming these barriers, unlocking the full potential of RTP materials in OLEDs and beyond. The future of RTP materials in optoelectronics is not just about enhancing device performance but also about redefining the principles of sustainable technology development.

AUTHOR CONTRIBUTIONS

Hui Li: Writing – original draft. **Cheng Chen:** Writing – review & editing. **Zongji Ye:** Writing – review & editing. **Kai Feng:** Writing – review & editing. **Jiani Huang:** Writing – review & editing. **Gaozhan Xie:** Writing – original draft; Writing – review & editing. **Ye Tao:** Conceptualization; funding acquisition; project administration; writing – original draft; writing – review & editing.

ACKNOWLEDGMENTS

This study was supported in part by the Open Research Fund of Songshan Lake Materials Laboratory (2022SLABFN16), the National Natural Science Foundation of China (22075149, 22322106, 62075102, 22105104, and 62288102), Project of State Key Laboratory of Organic Electronics and Information Displays, Nanjing University of Posts and Tele-communications, (No. GDX2024010002), and the Hua Li Talents Program of Nanjing University of Posts and Telecommunications.

CONFLICT OF INTEREST STATEMENT

The authors declare no conflict of interests.

DATA AVAILABILITY STATEMENT

Data sharing is not applicable to this article as no new data were created or analyzed in this study.

ORCID

Hui Li  <https://orcid.org/0000-0002-5080-2533>

REFERENCES

1. R. Kabe, C. Adachi, *Nature* **2017**, 550, 384.
2. J. Yang, X. Zhen, B. Wang, X. Gao, Z. Ren, J. Wang, Y. Xie, J. Li, Q. Peng, K. Pu, Z. Li, *Nat. Commun.* **2018**, 9, 840.
3. S. A. Fateminia, Z. Mao, S. Xu, Z. Yang, Z. Chi, B. Liu, *Angew. Chem. Int. Ed.* **2017**, 129, 12328.
4. P. Cen, J. Huang, C. Jin, J. Wang, Y. Wei, H. Zhang, M. Tian, *Aggregate* **2023**, 4, e352.
5. G. Xiao, Y. Ma, Z. Qi, X. Fang, T. Chen, D. Yan, *Chem. Sci.* **2024**, 15, 3625.3632
6. C. Xing, B. Zhou, D. Yan, W. Fang, *CCS Chem* **2023**, 5, 2866.
7. C. Xing, Z. Qi, B. Zhou, D. Yan, W. H. Fang, *Angew. Chem. Int. Ed.* **2024**, 63, e202402634.
8. C. Xing, B. Zhou, D. Yan, W. H. Fang, *Adv. Sci.* **2024**, 11, 2310262.
9. K. Jiang, L. Zhang, J. Lu, C. Xu, C. Cai, H. Lin, *Angew. Chem. Int. Ed.* **2016**, 55, 7231.
10. Z. Liu, D. Li, L. Tong, Y. Meng, M. Fang, J. Yang, B. Z. Tang, Z. Li, *Adv. Opt. Mater.* **2023**, 11, 2203069.
11. Q. Feng, Z. Xie, M. Zheng, *Sens. Actuators B Chem.* **2022**, 351, 130976.
12. Z. Chen, X. Liang, D. He, M. Hu, L. Wen, *New J. Chem.* **2023**, 47, 12688.
13. H. Hu, J. Li, X. Gong, *Small* **2023**, 2308457.
14. C. Adachi, M. A. Baldo, M. E. Thompson, S. R. Forrest, *J. Appl. Phys.* **2001**, 90, 5048.
15. Y. Yang, K. Wang, D. Yan, *ACS Appl. Mater. Inter.* **2016**, 8, 15489.
16. M. Schulze, A. Steffen, F. Würthner, *Angew. Chem. Int. Ed.* **2015**, 54, 1570.
17. Z. Wu, J. Nitsch, T. B. Marder, *Adv. Opt. Mater.* **2021**, 9, 2100411.
18. L. Xiao, H. Fu, *Chem. Eur. J.* **2019**, 25, 714.
19. V. V. Patil, C. L. Kim, D. R. Lee, J. Y. Lee, Y. Kang, *Dyes Pigm.* **2022**, 207, 110741.
20. X. Yang, S. Wang, K. Sun, H. Liu, M. Ma, S. T. Zhang, B. Yang, *Angew. Chem. Int. Ed.* **2023**, 62, e202306475.

21. Y. He, J. Wang, Q. Li, S. Qu, C. Zhou, C. Yin, H. Ma, H. Shi, Z. Meng, Z. An, *Adv. Opt. Mater.* **2023**, *11*, 2201641.
22. Q. Yu, J. Zhang, J. W. Lam, D. Yang, J. Sun, B. Z. Tang, *ACS Mater. Lett.* **2023**, *5*, 2691.
23. I. Bhattacharjee, N. Acharya, S. Karmakar, D. Ray, *J. Phys. Chem. C* **2018**, *122*, 21589.
24. G. Yin, W. Lu, J. Huang, R. Li, D. Liu, L. Li, R. Zhou, G. Huo, T. Chen, *Aggregate* **2023**, *4*, e344.
25. M. Gutiérrez, C. Martín, J. Hofkens, J. Tan, *J. Mater. Chem. C* **2021**, *9*, 15463.
26. H. Yuasa, S. Kuno, *B. Chem. Soc. Jpn.* **2018**, *91*, 223.
27. W. Li, W. Zhou, Z. Zhou, H. Zhang, X. Zhang, J. Zhuang, Y. Liu, B. Lei, C. Hu, *Angew. Chem. Int. Ed.* **2019**, *131*, 7356.
28. B. Zhou, Z. Qi, M. Dai, C. Xing, D. Yan, *Angew. Chem. Int. Ed.* **2023**, *135*, e202309913.
29. Y. Zhang, S. Zhang, G. Liu, Q. Sun, S. Xue, W. Yang, *Chem. Sci.* **2023**, *14*, 5177.
30. X. Fang, Y. Tang, Y. Ma, G. Xiao, P. Li, D. Yan, *Sci. China Mater.* **2023**, *66*, 664.
31. Y. Zhang, X. Chen, J. Xu, Q. Zhang, L. Gao, Z. Wang, L. Qu, K. Wang, Y. Li, Z. Cai, Y. Zhao, C. Yang, *J. Am. Chem. Soc.* **2022**, *144*, 6107.
32. J. Yuan, Z. Li, J. Chen, Y. Qi, P. Li, T. Yu, Y. Tao, R. Chen, *J. Mater. Chem. C* **2023**, *11*, 113.
33. J. Yuan, S. Wang, Y. Ji, R. Chen, Q. Zhu, Y. Wang, C. Zheng, Y. Tao, Q. Fan, W. Huang, *Mater. Horiz.* **2019**, *6*, 1259.
34. Y. Gong, L. Zhao, Q. Peng, D. Fan, W. Z. Yuan, Y. Zhang, B. Z. Tang, *Chem. Sci.* **2015**, *6*, 4438.
35. C. Wang, Y. Gong, W. Yuan, Y. Zhang, *Chin Chem Lett* **2016**, *27*, 1184.
36. S. Xiong, Y. Xiong, D. Wang, Y. Pan, K. Chen, Z. Zhao, D. Wang, B. Z. Tang, *Adv. Mater.* **2023**, *35*, 2301874.
37. C. Zhang, L. Lou, Y. Li, S. Sun, W. Hu, K. Wang, D. Wang, H. Cao, W. He, Z. Yang, *J. Phys. Chem. C* **2023**, *127*, 20929.
38. J. Chen, F. Lin, G. Liang, H. Huang, T. Qin, Z. Yang, Z. Chi, *J. Mater. Chem. C* **2023**, *11*, 6290.
39. Y. Si, Y. Zhao, W. Dai, S. Cui, P. Sun, J. Shi, B. Tong, Z. Cai, Y. Dong, *Chin J. Chem* **2023**, *41*, 1575.
40. Y. Xia, C. Zhu, F. Cao, Y. Shen, M. Ouyang, Y. Zhang, *Angew. Chem. Int. Ed.* **2023**, *135*, e202217547.
41. Y. Tian, J. Yang, Z. Liu, M. Gao, X. Li, W. Che, M. Fang, Z. Li, *Angew. Chem. Int. Ed.* **2021**, *60*, 20259.
42. C. Xia, S. Zhu, S. Zhang, Q. Zeng, S. Tao, X. Tian, Y. Li, B. Yang, *ACS Appl. Mater. Inter.* **2020**, *12*, 38593.
43. C. Zheng, S. Tao, B. Yang, *Small Struct.* **2023**, *4*, 2200327.
44. G. Bergamini, A. Fermi, C. Botta, U. Giovanella, S. Di Motta, F. Negri, R. Peresutti, M. Gingras, P. Ceroni, *J. Mater. Chem. C* **2013**, *1*, 2717.
45. P. Anzenbacher, C. Pérez-Bolívar, S. Takizawa, V. Brega, *J. Lumin.* **2016**, *180*, 111.
46. R. Kabe, N. Notsuka, K. Yoshida, C. Adachi, *Adv. Mater.* **2015**, *28*, 655.
47. Y. He, N. Cheng, X. Xu, J. Fu, J. Wang, *Org. Electron.* **2019**, *64*, 247.
48. J. Wang, J. Liang, Y. Xu, B. Liang, J. Wei, C. Li, X. Mu, K. Ye, Y. Wang, *J. Phys. Chem. C* **2019**, *10*, 5983.
49. T. Wang, X. Su, X. Zhang, X. Nie, L. Huang, X. Zhang, X. Sun, Y. Luo, G. Zhang, *Adv. Mater.* **2019**, *31*, 1904273.
50. C. L. Kim, J. Kim, H. Jang, D. R. Lee, J. Y. Lee, *ACS Appl. Energ. Mater.* **2022**, *5*, 4985.
51. Z. Chen, M. Li, Q. Gu, X. Peng, W. Qiu, W. Xie, D. Liu, Y. Jiao, K. Liu, J. Zhou, S. Su, *Adv. Sci.* **2023**, *10*, 2207003.
52. W. Qiu, D. Liu, Z. Chen, Y. Gan, S. Xiao, X. Peng, D. Zhang, X. Cai, M. Li, W. Xie, G. Sun, Y. Jiao, Q. Gu, D. Ma, S. J. Su, *Matter* **2023**, *6*, 1231.
53. G. Zhan, Z. Liu, Z. Bian, C. Huang, *Front. Chem.* **2019**, *7*, 305.
54. M. S. Lodge, S. A. Yang, S. Mukherjee, B. Weber, *Adv. Mater.* **2021**, *33*, 2008029.
55. D. Lee, O. Bolton, B. C. Kim, J. H. Youk, S. Takayama, J. Kim, *J. Am. Chem. Soc.* **2013**, *135*, 6325.
56. L. Y. Liang, B. B. Chen, Y. Wang, Y. T. Gao, S. Chang, M. L. Liu, *J. Colloid Interf. Sci.* **2023**, *649*, 445.
57. Z. Xu, Y. He, H. Shi, Z. An, *SmartMat* **2023**, *4*, e1139.
58. M. Hayduk, S. Riebe, J. Voskuhl, *Chem. Eur. J.* **2018**, *24*, 12221.
59. Y. Li, L. Jiang, W. Liu, S. Xu, T. Y. Li, F. Fries, O. Zeika, Y. Zou, C. Ramanan, S. Lenk, R. Scholz, D. Andrienko, X. Feng, K. Leo, S. Reineke, *Adv. Mater.* **2021**, *33*, 2101844.
60. M. Fang, J. Yang, Z. Li, *Chin J. Polym Sci* **2019**, *37*, 383.
61. W. Zhao, Z. He, B. Z. Tang, *Nat. Rev. Mater.* **2020**, *5*, 869.
62. L. Ma, X. Ma, *Sci. China Chem.* **2023**, *66*, 304.
63. S. Xu, R. Chen, C. Zheng, W. Huang, *Adv. Mater.* **2016**, *28*, 9920.
64. B. Zhou, D. Yan, *Adv. Funct. Mater.* **2023**, *33*, 2300735.
65. B. Song, W. Shao, J. Jung, S. Yoon, J. Kim, *ACS Appl. Mater. Inter.* **2020**, *12*, 6137.
66. D. R. Lee, S. H. Han, J. Y. Lee, *J. Mater. Chem. C* **2020**, *7*, 11500.
67. D. R. Lee, K. H. Lee, W. Shao, C. L. Kim, J. Kim, J. Y. Lee, *Chem. Mater.* **2020**, *32*, 2583.
68. Z. Chen, Q. Gu, M. Li, W. Qiu, Y. Jiao, X. Peng, W. Xie, D. Liu, K. Liu, Z. Yang, *Adv. Opt. Mater.* **2024**, 2302503.
69. H. Chen, Y. Deng, X. Zhu, L. Wang, L. Lv, X. Wu, Z. Li, Q. Shi, A. Peng, Q. Peng, Z. Shuai, Z. Zhao, H. Chen, H. Huang, *Chem. Mater.* **2020**, *32*, 4038.
70. W. Qiu, X. Cai, Z. Chen, X. Wei, M. Li, Q. Gu, X. Peng, W. Xie, Y. Jiao, Y. Gan, W. Liu, S. Su, *J. Phys. Chem. L* **2022**, *13*, 4971.
71. M. Li, W. Xie, X. Cai, X. Peng, K. Liu, Q. Gu, J. Zhou, W. Qiu, Z. Chen, Y. Gan, S. J. Su, *Angew. Chem. Int. Ed.* **2022**, *61*, e202209343.
72. J. Sun, J. Jia, B. Zhao, J. Yang, M. Singh, Z. An, H. Wang, B. Xu, W. Huang, *Chinese Chem. Lett.* **2021**, *32*, 1367.
73. K. Tabata, T. Yamada, H. Kita, Y. Yamamoto, *Adv. Funct. Mater.* **2019**, *29*, 1805824.
74. C. Chen, R. Huang, A. S. Batsanov, P. Pander, Y. T. Hsu, Z. Chi, F. B. Dias, M. R. Bryce, *Angew. Chem. Int. Ed.* **2018**, *57*, 16407.
75. P. Data, M. Okazaki, S. Minakata, Y. Takeda, *J. Mater. Chem. C* **2019**, *7*, 6616.
76. H. F. Higginbotham, M. Okazaki, P. de Silva, S. Minakata, Y. Takeda, P. Data, *ACS Appl. Mater. Inter.* **2021**, *13*, 2899.
77. T. Hosono, N. O. Decarli, P. Z. Crocomo, T. Goya, L. E. de Sousa, N. Tohnai, S. Minakata, P. de Silva, P. Data, Y. Takeda, *J. Mater. Chem. C* **2022**, *10*, 4905.
78. D. R. L. N. Daniel De Sa Pereiral, A. S. B. J. Long Kim, Daniel De Sa Pereira, *J. Mater. Chem. C* **2019**, *37*, 11317.
79. C. L. Kim, J. Jeong, D. R. Lee, H. J. Jang, S. Kim, M. Baik, J. Y. Lee, *J. Phys. Chem. L* **2020**, *11*, 5591.
80. A. Tomkeviciene, M. M. G. V. Tomas, J. V. Grazulevicius, V. Andruleviciene, D. Volyniuk, *Org. Electron* **2019**, *70*, 227.
81. D. Chaudhuri, E. Sigmund, A. Meyer, L. Röck, P. Klemm, S. Lautenschlager, A. Schmid, S. R. Yost, T. Van Voorhis, S. Bange, S. Höger, J. M. Lupton, *Angew. Chem. Int. Ed.* **2013**, *52*, 13449.

82. J. Wang, B. Liang, J. Wei, Q. Li, Y. Xu, T. Yang, C. Li, Y. Wang, *Angew. Chem. Int. Ed.* **2021**, *28*, 15335.
83. G. Xie, J. Wang, X. Xue, H. Li, N. Guo, H. Li, D. Wang, M. Li, W. Huang, R. Chen, Y. Tao, *Appl. Phys. Rev.* **2022**, *9*, 031410.
84. C. Si, T. Wang, A. K. Gupta, D. B. Cordes, A. M. Z. Slawin, J. S. Siegel, E. Z. Colman, *Angew. Chem. Int. Ed.* **2023**, *62*, e202309718.
85. J. Tan, W. Chen, S. Ni, Z. Qiu, Y. Zhan, Z. Yang, J. Xiong, C. Cao, Y. Huo, C. Lee, *J. Mater. Chem. C* **2020**, *8*, 8061.
86. X. Wu, C. Huang, D. Chen, D. Liu, C. Wu, K. Chou, B. Zhang, Y. Wang, Y. Liu, E. Y. Li, W. Zhu, P. Chou, *Nat. Commun.* **2020**, *11*, 2145.
87. X. Liu, L. Yang, X. Li, L. Zhao, S. Wang, Z. H. Lu, J. Ding, L. Wang, *Angew. Chem. Int. Ed.* **2020**, *60*, 2455.2463.

AUTHOR BIOGRAPHIES



Hui Li obtained bachelor's degree from Quzhou University in 2021. He is currently a master's student under the supervision of Prof. Ye Tao at Nanjing University of Posts and Telecommunications. His research interests primarily focus on afterglow organic light-emitting diodes.



Gaozhan Xie received his Bachelor's degree from Southwest University in Chongqing. He obtained his Master's degree in materials science and engineering from South China University of Technology in Guangzhou under the supervision of Prof. Shi-Jian Su. He received his PhD

degree in organic chemistry from Ruprecht-Karls Universität Heidelberg in Germany under the supervision of Prof. Uwe H. F. Bunz. Then he joined the faculty of Nanjing University of Posts and Telecommunications in 2020. His present interests are in the development of organic optoelectronic materials and devices.



Ye Tao received his Bachelor's degree from Anhui University of Science and Technology, after which he obtained a PhD degree from Nanjing University of Posts and Telecommunications under the supervision of Prof. Wei Huang and Prof. Runfeng Chen. Later, he moved to Nanyang Technological University to do his postdoctoral research with Professor Qi Jie Wang. In 2018, he obtained a professor position in Nanjing University of Posts and Telecommunications. His main research interests focus on organic functional materials and devices.

How to cite this article: H. Li, C. Chen, Z. Ye, K. Feng, J. Huang, G. Xie, Y. Tao, *FlexMat* **2024**, *1*, 173. <https://doi.org/10.1002/flm2.23>